Aus der Medizinischen Klinik mit Schwerpunkt Nephrologie und
internistische Intensivmedizin der Medizinischen Fakultät
der Charité–Universitätsmedizin Berlin

DISSERTATION

# Structural and functional basis of Endothelin-1 type A receptor ($ET_AR$) activation

zur Erlangung des akademischen Grades
Doctor medicinae (Dr. med.)

vorgelegt der Medizinischen Fakultät
Charité – Universitätsmedizin Berlin

von

Sumin Wu
aus Neimenggu, China

Datum der Promotion: 01.03.2019

# Table of contents

# ABBREVIATIONS

| | |
|---|---|
| Ala | Alanine |
| AR | Adrenergic receptor |
| ASK1 | Apoptosis-signal regulation kinase 1 |
| Asn | Asparagine |
| $AT_1R$ | Angiotensin II type 1 receptor |
| $AT_1R$-IgG | IgG targeting $AT_1R$ |
| bp | Base pair |
| cAMP | Cyclic adenosine monophosphate |
| CAMs | Constitutively active mutants |
| CCL 18 | Chemokine ligand 18 |
| cDNA | Complementary DNA |
| Conc. | concentration |
| Cys | Cysteine |
| DNA | Deoxyribonucleic acid |
| ECE | Endothelin-converting enzyme |
| ECL | Extracellular loop |
| ERK1/2 | Extracellular signal-regulated kinases 1 and 2 |
| ET-1 | Endothelin-1 |
| ET-2 | Endothelin-2 |
| ET-3 | Endothelin-3 |
| $ET_AR$ | Endothelin-1 type A receptor |
| $ET_AR$-IgG | IgG targeting $ET_AR$ |
| $ET_BR$ | Endothelin-1 type B receptor |
| GAPDH | Glyceraldehyde 3-phosphate dehydrogenase |
| GFP | Green fluorescent protein |
| Gln | Glutamine |
| Gly | Glycine |
| GPCR | G-protein coupled receptor |
| His | Histidine |
| HMEC | Human microvascular endothelial cell |
| IgG | Immunoglobulin class G |

| | |
|---|---|
| IL-8 | Interleukin 8 |
| JNK | c-Jun kinase |
| kD | Kilodalton |
| Lys | Lysine |
| M | Molar |
| MAPK | Mitogen-activated protein kinase |
| MEKK1 | MAPK kinase kinase 1 |
| mL | Milliliter |
| mRNA | Messenger RNA |
| NFAT | Nuclear factor of activated T-cells |
| nm | Nanometer |
| PAH | Pulmonary arterial hypertension |
| PBS | Dulbecco's phosphate buffered saline |
| PCR | Polymerase chain reaction |
| Phe | Phenylalanine |
| PKC | Protein kinase C |
| qRT-PCR | Quantitative Real Time-PCR |
| RNA | Ribonucleic acid |
| ROCK | Rho-associated protein kinase |
| RT | Reverse transcription |
| SD | Standard deviation |
| SEM | Standard error of the mean |
| SRF | Serum response factor |
| SSc | Systemic sclerosis |
| ssDNA | Single-strand DNA |
| TGF-β | Transforming growth factor beta |
| TM | Transmembrane |
| Trp | Tryptophan |
| TSH | Thyrotropin, thyroid stimulating hormone |
| TSHR | Thyroid stimulating hormone receptor |
| Tyr | Tyrosine |
| V | Voltage |
| WT | Wild type |

| | |
|---|---|
| $\alpha_{1a}$AR | Alpha-1A adrenergic receptor |
| $\beta_1$AR | Beta-1 adrenergic receptor |
| $\beta_2$AR | Beta-2 adrenergic receptor |
| μg | Microgram |
| μL | Microliter |

# Abstract

Endothelin-1 type A ($ET_AR$) and B receptors ($ET_BR$) belong to the GPCR subfamily A and mediate the actions of their peptide agonist Endothelin-1 (ET-1). ET-1 is one of the most potent vasoconstrictors in the human organism and regulates blood pressure and local and systemic homeostasis. $ET_AR$ can be activated not only by ET-1 but also by agonistic antibodies. As recently demonstrated, extracellular binding of agonistic autoantibodies targeting $ET_AR$ ($ET_AR$-IgG) promotes downstream signaling through allosteric activation of the receptor, independent of ET-1. The resultant signaling induced severe renovascular disease, exemplified on systemic sclerosis related renal crisis (SSc). Despite their clinical relevance, the potential differences and similarities to natural ligand-mediated activation have not been studied yet.

To investigate relevant extracellular loops required for ET-1 and $ET_AR$-IgG binding and downstream signaling responses, each of the three extracellular loops (ECL) was individually mutated. Functional effects were assessed with two different assays. The first GPCR activation assay relied on the MMY yeast model, in which a single human GPCR controls yeast growth to assess the effects of the mutations on $ET_AR$-IgG-mediated $ET_AR$ activation. In the second assay, luciferase reporter plasmids enabled monitoring of G-proteins binding to $ET_AR$ in response to ET-1 and $ET_AR$-IgG.

Change of ECL3 structure resulted in the constitutive activation of $ET_AR$ both in MMY yeast model and in luciferase reporter assays. Besides, mutating ECL1 to Alanine or replacing ECL2 demonstrated no effect on $ET_AR$-IgG -induced $ET_AR$ activation in yeast GPCR activation assay. In addition, these mutations did not influence $ET_AR$-IgG -mediated $G_{q/11}$ and $G_{12/13}$ binding to $ET_AR$ as revealed by luciferase reporter assays. On the contrary, results showed that intact structure of ECL1 and ECL2 is necessary for $G_{12/13}$ activation upon ET-1 stimulation.

This work demonstrates that unlike similar antibodies against other GPCRs, antibodies directed against Endothelin-1 type A receptor do not bind to the extracellular loops of the receptor; thereby eliciting intracellular signaling differences from the natural ligand. Elucidation of these epitopes

is a prerequisite for rational design of new potent and more precise pharmacological compounds to replace old, relatively inefficient ones.

# Abstrakt

Endothelin-1 Typ A ($ET_AR$) und B Rezeptoren ($ET_BR$) gehören zur Unterfamilie A der GPCR und vermitteln die Signale ihres Peptidagonisten Endothelin-1 (ET-1). ET-1 ist einer der stärksten Vasokonstriktoren im menschlichen Organismus und reguliert Blutdruck und lokale und systemische Homöostase. $ET_AR$ können nicht nur durch ET-1 aktiviert werden, sondern auch durch agonistische Antikörper. Wie vor kurzem gezeigt, induziert die extrazelluläre Bindung agonistischer Autoantikörper am $ET_AR$ ($ET_AR$-IgG) downstream Signaling durch allosterische Rezeptoraktivierung unabhängig von ET-1. Dadurch können schwere renovaskuläre Erkrankungen ausgelöst werden, wie sich am Beispiel der renalen Krise bei Systemischer Sklerose (SSc) zeigt. Trotz ihrer klinischen Bedeutung, wurden die möglichen Unterschiede und Ähnlichkeiten zur Rezeptoraktivierung durch den natürlichen Liganden bisher noch nicht erforscht. Um die für die Bindung von ET-1 und der $ET_AR$-IgG entscheidenden extrazellulären Schleifen und intrazelluläre Signalantworten untersuchen zu können, wurden jede der drei extrazellulären Schleifen (ECL) einzeln mutiert. Funktionelle Effekte wurden mit zwei verschiedenen Assays überprüft. Der erste GPCR Aktivierungsassay beruhte auf einem MMY Hefemodell, bei dem ein einzelner humaner GPCR das Hefewachstum bestimmt. Beim zweiten Assay ermöglichte ein Luziferase-Reporterplasmidassay, die Bindung von G-Proteinen an den $ET_AR$ nach Stimulation mit ET-1 und $ET_AR$-IgG zu monitoren.

Veränderungen an der Struktur der 3. ECL führten zur konstitutiven Aktivierung des $ET_AR$, sowohl im MMY Hefemodell, als auch im Luziferase-Reporterassay. Dagegen blieben die Mutation zu Alanin an der 1. ECL oder der Ersatz der 2. ECL ohne Wirkung auf die $ET_AR$-IgG -induzierte $ET_AR$ Aktivierung im Hefe GPCR Aktivierungsassay. Darüberhinaus beeinflussten diese Mutation die $ET_AR$-IgG vermittelte Bindung von $G_{q/11}$ und $G_{12/13}$ an den $ET_AR$ nicht, wie in Luziferase-Reporterassays gezeigt wurde. Im Gegensatz dazu zeigten die Ergebnisse, dass die intakten Strukturen der 1. ECL und 2. ECL für die $G_{12/13}$ Aktivierung durch ET-1 notwendig sind. Diese Arbeiten zeigen, dass anders als bei ähnlichen GPCR-Antikörpern, die gegen den Endothelin-1 type A Rezeptor gerichtete Antiköper nicht an die extrazellulären Rezeptorschleifen

binden. Dadurch ergeben sich Unterschiede zum intrazellulären Signaling des natürlichen Liganden. Die Aufklärung der Bindungsepitope ist die Voraussetzung für die Entwicklung neuer, präziser und wirksamerer Medikamente, um die alten, relativ ineffizienten Arzneien zu ersetzen.

# 1 Introduction

## 1.1 Endothelin-1 receptors

G-protein-coupled receptors (GPCR), also known as 7-transmembrane receptors (7-TM), comprise the largest receptor family and the most important drug targets, since more than 40% of currently used drugs are GPCR modulators. More than 800 human GPCRs are clustered into five different classes: rhodopsin, secretin, adhesion, glutamate and frizzled / taste2 [1]. GPCRs transduce signals elicited by their endogenous ligands, which range from vasoactive peptides, neurotransmitters, chemokines, hormones and fatty acids to physical stimuli such as light [2]. Endothelin receptors, Endothelin-1 type A ($ET_AR$) and type B ($ET_BR$) receptors, belong to the class A GPCRs and interact in a similar manner with their natural peptide agonist ET-1, but yield different signals with a sequence similarity of 63% [3]. The localization of the two receptors is different. $ET_AR$ is localized in vascular smooth muscle, heart, lung and kidney, whereas $ET_BR$ can be found in more tissues, mainly in the brain, kidney, liver and lung [4]. ET receptors are susceptible to various factors and can be up- or downregulated. Hypoxia, cAMP, epidermal growth factor upregulate the $ET_AR$ production; Endothelins, Angiotensin II, platelet derived growth factor and TGF-β downregulate $ET_AR$ expression [5].

### 1.1.1 Endothelin-1 type A receptor

The gene coding for the human $ET_A$ receptor (*EDNRA*) is located on chromosome 4, which contains eight exons and seven introns [6]. The molecular weight of $ET_AR$ is about 44 kDa, consisting of 427 amino acids; its affinity for ET-1 is higher than for ET-2 and ET-3. Figure 1 shows the amino acid sequence and structure of $ET_AR$. Mutation of a cluster of five Cys residues into either serine or alanine in the cytoplasmic tail did not alter the binding but completely blocked palmitoylation of $ET_AR$, which led to a failure of ET-1 to increase the cytoplasmic calcium [7]. Deletion of either the entire extracellular N-terminus or the intracellular C-terminus completely inactivated ET-1 binding [8].

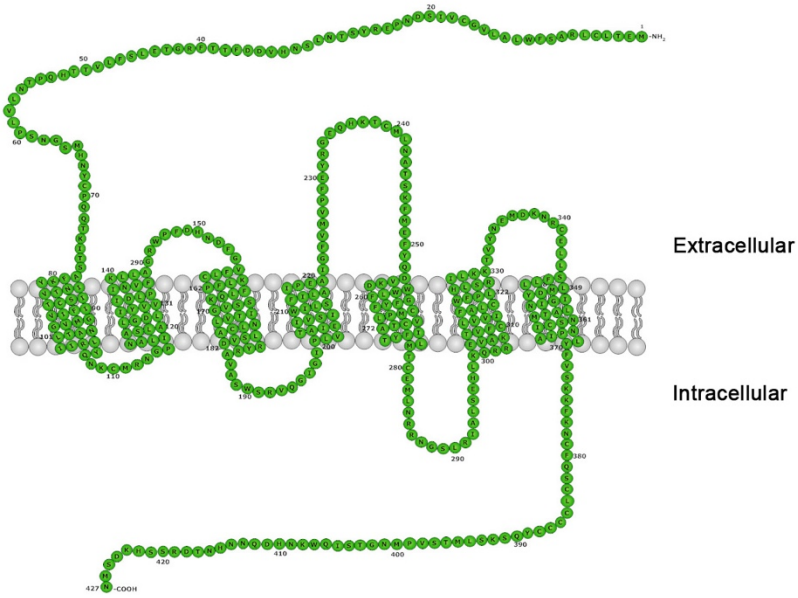


Figure 1. Schematic diagram of $ET_AR$.

Typical for a GPCR, the activation of $ET_AR$ can initiate downstream physiological and pathophysiological processes. Human $ET_AR$ can couple with $G_{q/11}$, $G_s$ and $G_{12/13}$. $ET_AR$ expressed at different levels in CHO cells provide evidence that the coupling of $ET_AR$ to $G_{q/11}$ and $G_{12/13}$ differs depending on the expression level of the receptor, resulting in the activation of different signaling cascades [9]. The precise signaling pathways responsible for endothelin-induced vasoconstriction are still being actively studied. However, it is widely accepted that the activation of phospholipase C, production of inositol triphosphate and mobilization of calcium are the most relevant factors. Except for the effects on vascular tone, Endothelins also promote the growth and proliferation of vascular smooth muscle cells, which appears to be $ET_AR$-mediated, involving the activation of mitogen-activated protein (MAP) kinases and the transactivation of epidermal growth factor receptor [10].

In 2016, crystal structure and conformational changes of human Endothelin-1 type B Receptor ($ET_BR$) with and without its ligand ET-1 was reported [11]. However, the crystal structure of $ET_AR$ remains unsolved. Due to the low expression levels and poor stability, crystallization and GPCRs structure determination studies are difficult to perform. Another way to study the structure of a GPCR is to change all amino acids of the GPCR individually or in a group. Amino acids are often replaced by Alanine, due to its high helix propensity and low probability of steric hindrance [12].

Such studies have been performed on $ET_AR$. Eighteen amino acids were mutated and analyzed for binding of Endothelin-1 and Bosentan, an inhibitor of both $ET_A$-and $ET_BR$. It has been observed that single point mutations differentially affect binding of agonist and antagonist [13]. In the N-terminus of $ET_AR$, two mutants containing D46N or R53Q substitutions showed dramatically reduced binding to ET-1, indicating that the substitutions of single amino acid alter the three-dimensional structure of the ligand-binding domain of the receptor [14]. Furthermore, it has been reported that Tyr129 is important for the peptide ligand affinity and selectivity of $ET_AR$ [15].

### 1.1.2 Endothelin-1 type B receptor

The gene coding for the human $ET_B$ receptor (*EDNRB*) is located on chromosome 13 and contains seven exons and six introns [16]. The molecular weight of $ET_BR$ is 32 kDa and consists of 442 amino acids with same affinity for the three Endothelins. In 2016, Shihoya and co-workers reported the amino acid sequence, crystal structure and conformational changes of $ET_BR$ in its ligand-free form and complexed with ET-1 [11]. When $ET_BR$ interacts with ET-1, the N-terminus, the three extracellular loops and six transmembrane helices (2-7) are fully occupied. $ET_BR$ has a fundamental role in renal, pulmonary, coronary, cerebral and systemic circulation. $ET_BR$ in the endothelium mediates the release of vessel relaxants such as nitric oxide, prostacyclin and endothelium-derived hyperpolarizing factors; it also plays an essential role in the clearance of ET-1 [17].

## 1.2 Endothelin-1, a natural peptide agonist of Endothelin-1 receptors

### 1.2.1 Synthesis of Endothelin-1

Endothelins are 21-amino acid peptides that are mainly produced in the endothelium and have a molecular weight of about 2.5 kDa. There are three isoforms (ET-1, ET-2 and ET-3), each with different gene and tissue distributions. In healthy individuals, there is a subtle balance between vasoconstriction and vasodilation, but when ET-1 is overexpressed, it can cause vascular diseases in various organ systems [18]. The gene coding for human ET-1 is located on chromosome 6 with

a total length of 1246 base pairs. This gene product is a 212-amino acid preproET that is first converted intracellularly into an inactive pro-endothelin peptide, after the signal peptide has been removed, and then, in the case of ET-1, into the 38-amino acid long bigET. The bigET is then finally converted into the active form of the peptide and a C-terminal fragment by the endothelin-converting enzyme (ECE) [19] (Figure 2).

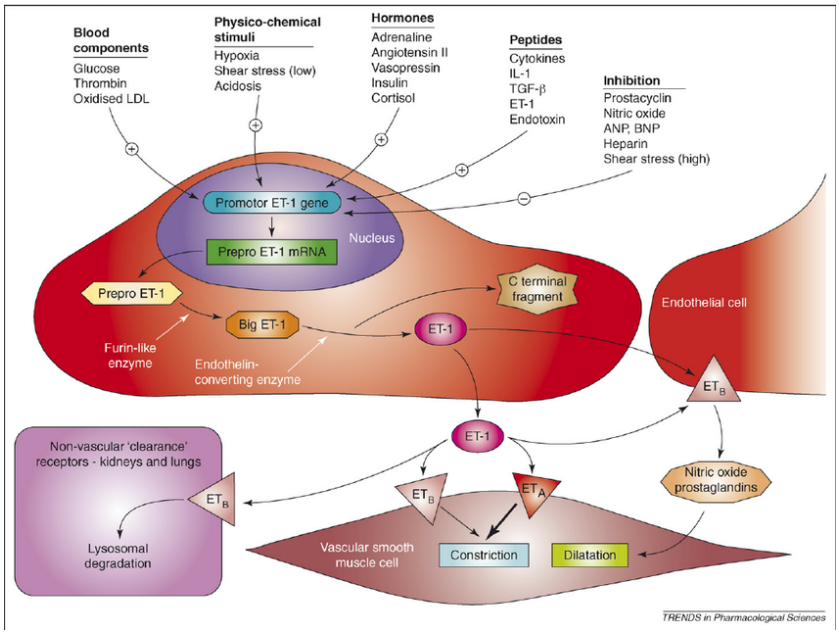


Figure 2. Pathways of endothelin-1 synthesis and sites of action [19]

Under normal physiological condition, the amount of circulating ET-1 is 0.26-5 ng/L [20], and ET-1 is eliminated from circulation with a half-life of one to seven minutes [21].

### 1.2.2 Physiological effects of Endothelin-1

ET-1 affects virtually every system that regulates blood pressure and local and systemic homeostasis. It is the strongest vasoconstrictor yet identified, at least 10-fold stronger than Angiotensin-II and 100-fold stronger than Norepinephrine [20]. The constrictor response caused by ET-1 can last for a considerable period, of several hours [22]. ET-1 plays a major role in the regulation of vascular function. Under physiological conditions, ET-1 induces sustained vasoconstriction of smooth muscle cells [23]. ET-1 maintains the basic vascular tone, modulates endothelin biosynthesis, and regulates water balance [24]. In the endothelin system, ET-1 regulates multiple renal functions like renal blood flow, glomerular filtration rate, salt and water excretion,

acid/base treatment and extracellular matrix accumulation [25]. ET-1 increases the release of superoxide anion products and cytokines, which contribute to the development of the inflammation [26], and it has also been shown to be involved in immune functions [27].

### 1.2.3 Structure of Endothelin-1

ET-1 adopts a bicyclic structure with two disulfide bonds consisting of four cysteines ($Cys^{1}$-$Cys^{15}$ and $Cys^{3}$-$Cys^{11}$) (Figure 3); it has six hydrophobic amino acids at its C-terminus called hydrophobic tail, both of which are important for ET-1 to maintain its activity. It has been shown that some residues at positions 18, 19 and 21 are crucial for ET-1 binding to the receptors. The deletion or substitution of Trp21 leads to the loss of receptor binding and activation [28]. An α-helical structure is formed between the central residues and the N-terminus, which is firmly attached to the α-helix through the disulfide bonds [3]. The N-terminus and α-helical regions of ET-1 have a fairly stable conformation, while the C-terminus is flexible and has an extended conformation [29].

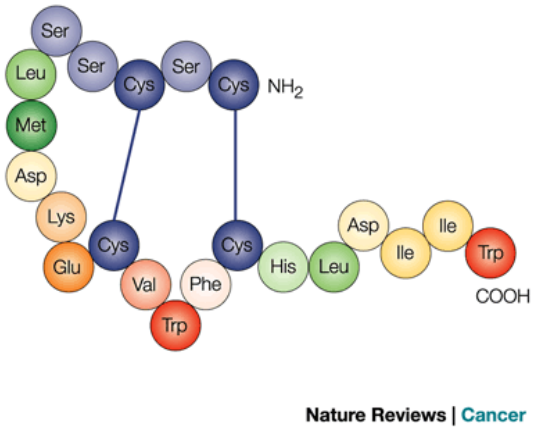


Figure 3. Amino-acid structure of ET-1 [30].

## 1.3 Autoantibodies targeting $ET_AR$

### 1.3.1 Autoantibodies targeting $ET_AR$ in obliterative vasculopathies

$ET_AR$ mediates the vasoconstrictive properties of ET-1 [31]. Functional autoantibodies have been involved in the pathogenesis of vascular lesions in renal and heart transplantation in the absence of donor specific-antibodies [32-34]. Banasik M *et al*. evaluated the presence of non-HLA antibodies (anti-Angiotensin II type 1 receptor ($AT_1R$) and/or anti-$ET_AR$) in 65 renal transplant patients. It was shown that 10.7% of the patients had a high level of non-HLA antibodies and graft loss in these patients was significantly higher. In another study conducted by the same group, the presence of $ET_AR$-IgG was evaluated in 116 renal transplant recipients. Anti-$ET_AR$ antibodies were observed in 47.4% of the patients and the function of the renal transplant was significantly worse in these patients. Hiemann *et al*. tested the impact of antibodies targeting $AT_1R$ and $ET_AR$ in 30 heart transplant recipients. They demonstrated that elevated levels of antibodies against $AT_1R$ and $ET_AR$ were associated with cellular and antibody-mediated rejection. $ET_AR$-IgG have also been involved in the pathogenesis of systemic sclerosis (SSc) [35].

### 1.3.2 Autoantibodies targeting $ET_AR$ in systemic sclerosis

#### 1.3.2.1 Clinical manifestations

Systemic sclerosis (SSc), also known as Scleroderma, is a chronic autoimmune and vascular disease of systemic connective tissue. Pulmonary and renal involvements are the leading causes of death in patients with SSc [36]. About 5-10% of diffuse SSc patients present with internal organ lesions at some point during the course of the disease and patients with greater and rapid skin lesions have the highest risk of developing renal complications [37]. Although therapies can alleviate some of the symptoms, there are no specific medications or therapies to reverse or control the progression of the disease.

#### 1.3.2.2 Pathogenesis and involvement of $ET_AR$-IgG

The difficulties in diagnosing and treating SSc are due to the complexity of the pathology of the disease, which involves interactions between the immune system, vascular system and connective tissue [38]. Extensive fibrosis, which is associated with diffuse small vessel vasculopathy, is unique and distinguishing in SSc [39]. Both vascular damage and activation of endothelial cells are prominent, and even occur before the fibrosis [40]. Microvasculature lesions involve mainly progressive thickening of the vessel wall, large gaps between endothelial cells, loss of vascular endothelium integrity, endometrial fibrosis, and hyperplasia, resulting in microthrombus formation leading to vascular occlusion and tissue hypoxia [41]. In addition, vascular repair and angiogenesis in SSc are found to be defective, leading to vasoconstriction and chronic clinical conditions in the affected area [42]. Several vasoactive peptides are involved in the pathogenesis of SSc, such as Endothelin-1[43]. Increased level of ET-1 has been reported in SSc patients [44] and elevated ET-1 levels are associated with renal failure [45]. Bosentan, an Endothelin-1 receptor blocker, can alleviate some of the vascular manifestations of SSc [46].

$ET_AR$-IgG were detected in most SSc patients with progressive vasculopathy; higher autoantibody levels were associated with more severe late complications and higher mortality [35]. This makes the detection and quantification of autoantibodies an important part of the diagnosis and treatment of SSc. $ET_AR$-IgG in SSc are not only associated with vascular complications, but may also be part of alloimmune and fibrotic complications that induce T cell migration and produce more interleukin 8 (IL-8) and chemokine ligand 18 (CCL18) [47]. *In vitro* $ET_AR$-IgG induced receptor-mediated ERK1/2 phosphorylation and increased TGF-β gene expression in HMECs [35]. $ET_AR$ antibodies increase endothelial $Ca^{2+}$ concentration and their action can be blocked *in vivo* by specific antagonist. In patient sera, anti-$ET_AR$ IgG are more common in SSc-associated pulmonary hypertension than in other forms of pulmonary arterial hypertension (PAH) [48].

# 2 Hypothesis and Objectives

## 2.1 Hypothesis

Autoantibodies targeting the Endothelin-1 type A receptor ($ET_AR$) have been detected in systemic sclerosis (SSc) and contribute to the pathogenesis of the disease and its clinical severity. Both the receptor natural peptide agonist, Endothelin-1 (ET-1), and antibodies targeting $ET_AR$ and isolated from SSc patients, $ET_AR$-IgG, activate $ET_AR$ and trigger downstream intracellular signaling. However, binding sites and downstream intracellular signaling might differ substantially between patients´ $ET_AR$-IgG and natural peptide agonist. A thorough knowledge of the cellular mechanisms of antibody-mediated receptor activation is necessary to provide further insights for the development of therapeutic strategies to block specifically the action of the antibodies and to understand specific pathways. Hence, the study aim of this thesis was to test the hypothesis that $ET_AR$-IgG isolated from SSc patients bind differently to $ET_AR$ as ET-1 with a binding occurring on the extracellular domains of the receptor and induce other cellular responses than the peptide agonist.

## 2.2 Objectives

1. To test the first hypothesis that $ET_AR$-IgG bind to extracellular domains of the receptor, different mutants of $ET_AR$ disturbing the structure of one of the three extracellular loops had to be created. Thus, ECL1 and -3 were mutated to Alanine to suppress folding and charge. To study ECL2, a construct, where ECL2 of $ET_AR$ has been replaced by Angiotensin II type 1 receptor ($AT_1R$) second extracellular loop, was already available in the laboratory [Development of a molecular toolbox to study the cross-talk between Angiotensin II type 1 and Endothelin-1 type A receptors in the context of obliterative vasculopathy, http://www.diss.fu-berlin.de/diss/receive/FUDISS_thesis_000000100230].

2. A GPCR activation assay already developed in the laboratory had to be optimized to study the binding of the antibodies to $ET_AR$ and the receptor´s activation in presence or absence of the ECLs mutations.

3. To investigate $ET_AR$-IgG effects on downstream signaling in comparison to natural peptide agonist ET-1, human microvascular endothelial cells (HMEC-1) were chosen as a mammalian cell model and luciferase reporter assays were performed to determine specific G-protein involvements.

# 3 Materials and methods

## 3.1 Materials

### 3.1.1 Chemical substances

| Chemicals and solutions | Manufacturer |
|---|---|
| 1 kb DNA ladder | Thermo Fisher Scientific |
| 2-Propanol | Carl Roth |
| 3-amino-1,2,4-triazole (3-AT) | Sigma |
| 5X Passive Lysis Buffer (PLB) | Promega |
| 10X M-MuLV Reverse Transcriptase Buffer | New England BioLabs |
| 10X Trypsin-EDTA | PAA |
| Agarose | Serva |
| Ampicillin | Alkom |
| Bacto Agar | BD |
| Bacto Peptone | BD |
| Bacto Trypton | BD |
| Bacto Yeast Extract | BD |
| Bis-Tris | AppliChem |
| Blasticidin S | InvivoGen |
| Dimethyl sulphoxide (DMSO) | Sigma Aldrich |
| dNTP mix | Thermo Fisher Scientific |
| Dulbecco's Modified Eagle's medium (DMEM) 4.5g/LGlucose | BioWest |
| DMEM 1.5 g/L Glucose | BioWest |
| Dulbecco’s Phosphate Buffered Saline (PBS) | Biochrom |

| Chemicals and solutions | Manufacturer |
|---|---|
| Dextrose (D(+)-Glucose) | Applichem |
| Ethylenediamintetra-acetic acid (EDTA) | Carl Roth |
| Ethanol 99.8% | Carl Roth |
| Ethanol 96% (MEK, denaturated) | Herbeta Arzneimittel |
| FastStart Universal SYBR Green Master | Roche |
| Fetal calf serum (FCS) | Gibco |
| Fluorescein-D-glucopyranoside (FDGlu) | Invitrogen |
| Gelatin | Sigma |
| Glycerin | Carl Roth |
| hEGF | Sigma Aldrich |
| Hydrocortisone | Sigma Aldrich |
| L-Glutamine | PAA |
| L-arginine (HCl) | Applichem |
| L-aspartic acid | Applichem |
| L-glutamic acid (monosodium) | Applichem |
| L-lysine monohydrate | Applichem |
| L-methionine | Applichem |
| L-phenylalanine | Applichem |
| L-serine | Applichem |
| L-threonine | Applichem |
| L-tyrosine | Applichem |
| L-valine | Applichem |
| L-histidine | Applichem |
| Lithium acetate | Applichem |
| MCDB-131 | c.c. pro GmbH |

| Chemicals and solutions | Manufacturer |
|---|---|
| Midori Green Advance DNA Stain | NIPPON Genetics |
| M-MuLV Reverse Transcriptase | New England BioLabs |
| NaCl Solution | Lonza |
| Oligo d(T) 16 | Invitrogen |
| PEG 3350 | Sigma Aldrich |
| Penicillin/Streptomycin (P/S) | PAA |
| RNase inhibitor | Thermo Fisher Scientific |
| SeaKem LE Agarose | Lonza |
| single-stranded DNA (ssDNA) | Sigma Aldrich |
| SOC Medium | Clontech |
| Sodium chloride | Carl Roth |
| Sodium hydroxide | Sigma Aldrich |
| Trypan blue | Sigma Aldrich |
| Tris | Carl Roth |
| Tris-HCl | Sigma Aldrich |
| Yeast nitrogen base without amino acids (AA) | Sigma Aldrich |

### 3.1.2 Equipment

| Equipment | Manufacturer |
|---|---|
| Applied Biosystems® 7500 Real-Time PCR System | Thermo Fisher Scientific |
| Axiovert 40 CFL Microscope | Carl Zeiss |
| Biofuge primo R | Thermo Fisher Scientific |
| Digital Heatblock II | VWR |
| FLUOstar OPTIMA Microplate Reader | BMG LABTECH |

| | |
|---|---|
| FRESCO 21 Centrifuge | Thermo Electron Corporation |
| HERA cell 240 Incubator | Thermo Electron Corporation |
| HERA safe Microbiological Safety Cabinet | Thermo Electron Corporation |
| Heraeus / BB 6220 CU $O_2$ | Thermo Fisher Scientific |
| Incubator B28 | BINDER |
| Incubating Orbital Shaker professional 3500 | VWR |
| ND-1000 Spectrophotometer | VWR |
| Perfusor secura FT | Braun |
| Polymax 1040 T Platform Shaker | Heidolph |
| SUB Waterbath | Grant |
| T Professional BASIC XL 96 Thermocycler | Biometra |
| UV-transilluminator Gene Flash | SYNGENE |

### 3.1.3 Kits

| **Kits** | **Manufacturer** |
|---|---|
| Direct-zol™ RNA MiniPrep | Zymo Research |
| GeneJET Plasmid Miniprep Kit | Thermo Fisher Scientific |
| HiTrap Protain G HP | GE Healthcare |
| In-Fusion ® HD Cloning Kit | Takara |
| Luciferase Assay System | Promega |
| NucleoBond®Xtra Midi/Maxi | Takara |
| NucleoBond®Xtra Midi/Maxi EF | Takara |
| PeqGOLD MicroSpin Cycle pure Kit | PEQLAB |
| Q5® Site-Directed Mutagenesis Kit | New England BioLabs |
| Xfect Transfection Reagent | Takara |

### 3.1.4 Plasmid, bacteria, cell line, yeast strains and enzymes

| **Plasmid** | **Manufacturer** |
|---|---|
| p426 GPD | GlaxoSmithKline |
| pcDNA3 | Thermo Fisher Scientific |
| pGL4.30 | Promega |
| pGL4.34 | Promega |

| **Bacteria** | **Manufacturer** |
|---|---|
| NEB 5-alpha Competent *E.coli* Cells | New England BioLabs |
| Stellar competent Cells | Takara |

| **Cell line** | **Manufacturer** |
|---|---|
| Human Microvascular Endothelial Cells (HMEC-1) | Kindly given by Dr. H.D. Orzechowski |

| **Yeast strains** | **Manufacturer** |
|---|---|
| MMY 12 | GlaxoSmithKline |
| MMY 14 | GlaxoSmithKline |

| **Enzymes and provided buffer** | **Manufacturer** |
|---|---|
| *Hind*III-HF | New England BioLabs |
| *Xho*I | New England BioLabs |
| CutSmart Buffer | New England BioLabs |

### 3.1.5 Agonist

| Agonist | Manufacturer |
|---|---|
| Endothelin 1 human and porcine | Sigma Aldrich |

### 3.1.6 Buffer recipes

| Buffer | Reagent | Final conc. |
|---|---|---|
| 3-AT | 3-amino-1,2,4-triazole | 1 M |
| | In $H_2O$ | |
| 50% PEG | PEG3350 | 50% m/v |
| | In $H_2O$ | |
| | Filtered (0.45 µm) | |
| Ampicillin stock solution | Ampicillin powder | 100 mg/mL |
| | In $H_2O$ | |
| | Filter sterilized (0.22 µm) | |
| Binding buffer, pH 7.0 | $Na_2HPO_4$ | 20 mM |
| | In $H_2O$ | |
| | Filtered (0.45 µm) | |
| BU salts 10X, pH 7.0 | $Na_2HP0_4·7H2O$ | 7% m/v |
| | $NaH_2PO_4$ | 3% m/v |
| | In $H_2O$ | |
| | Sterilized by autoclaving | |
| DNA sample loading buffer 6x | Glycerol | 30% v/v |
| | Xylene cyanole | 0.25% v/v |
| | Bromphenolblue | 0.25% m/v |

| Buffer | Reagent | Final conc. |
|---|---|---|
| | In $H_2O$ | |
| Elution buffer, pH 2.7 | Glycin-HCl | 0.1 M |
| | In $H_2O$ | |
| | Filtered (0.45 µm) | |
| Gelatin stock solution | gelatin | 2% m/v |
| | In PBS | |
| | Sterilized by autoclaving | |
| Histidine 100X | L-Histidine | 2 mg/mL |
| | In $H_2O$ | |
| | Filter sterilized (0.22 µm) | |
| LiAc | Lithium acetate | 1 M |
| | In $H_2O$ | |
| | Filter sterilized (0.22 µm) | |
| LiAc-TE | LiAc | 0.1 M |
| | TE 10x | 10%v/v |
| | In $H_2O$ | |
| LiAc-PEG-TE | LiAc | 0.1 M |
| | TE 10x | 10%v/v |
| | 50% PEG | 80% v/v |
| Neutralization buffer, pH 9.0 | Tris-HCl | 1 M |
| | In $H_2O$ | |
| | Filtered (0.45 µm) | |
| PBS ($Ca^{2+}$- /$Mg^{2+}$ -free), pH 7.3 | NaCl | 137 mM |
| | KCl | 2.7 mM |
| | $Na_2HPO_4$ | 9 mM |

| Buffer | Reagent | Final conc. |
|---|---|---|
| | $KH_2PO_4$ | 2.3 mM |
| | In $H_2O$ | |
| | Sterilized by autoclaving | |
| PLB 1X | PLB 5X | 20%v/v |
| | In $ddH_2O$ | |
| TBE buffer 1X, pH 8.0 | Tris | 89 mM |
| | Boric acid | 89 mM |
| | EDTA | 2 mM |
| | In $H_2O$ | |
| TE buffer 10X | Tris-HCl, pH 7.5 | 0.1 M |
| | EDTA | 0.01 M |
| | In $H_2O$ | |

### 3.1.7 Media

**Bacteria media**

| Lysogeny broth (LB) medium | Conc. |
|---|---|
| Bacto tryptone | 1% m/v |
| Bacto yeast extract | 0.5% m/v |
| NaCl | 1% m/v |
| | add Milli-Q water |
| Sterilize by autoclaving | |

| LB agar | Conc. |
|---|---|
| Bacto tryptone | 1% m/v |
| Bacto yeast extract | 0.5% m/v |

| | |
|---|---|
| NaCl | 1% m/v |
| Bacto agar | 1.5% m/v |
| | add Milli-Q water |

Sterilize by autoclaving

**Cell culture media**

| **Complete medium** | **Conc.** |
|---|---|
| L-glutamine | 10 mM |
| hEGF | 10 ng/mL |
| Hydrocortisone | 10 nM |
| FCS | 5% v/v |
| Penicillin | 100 U/mL |
| Streptomycin | 100 µg/mL |
| | add MCDB-131 |

| **Starvation medium** | **Conc.** |
|---|---|
| L-glutamine | 10 mM |
| hEGF | 10 ng/mL |
| Hydrocortisone | 10 nM |
| FCS | 0.5% v/v |
| Penicillin | 100 U/mL |
| Streptomycin | 100 µg/mL |
| | add MCDB-131 |

**Yeast media**

| **WHAUL powder** | **Conc.** |
|---|---|
| L-arginine (HCl) | 1.2 g |

| | |
|---|---|
| L-aspartic acid | 6.0 g |
| L-glutamic acid (monosodium) | 6.0 g |
| L-lysine | 1.8 g |
| L-methionine | 1.2 g |
| L-phenylalanine | 3.0 g |
| L-serine | 22.5 g |
| L-threonine | 12 g |
| L-tyrosine | 1.8 g |
| L-valine | 9.0 g |

| **40% Glucose** | **Conc.** |
|---|---|
| Dextrose | 40% m/v |
| Filtered (0.45 μm) | |

| **YNB 10X** | **Conc.** |
|---|---|
| yeast nitrogen base without AA | 6.7% m/v |
| Filter sterilized (0.22 μm) | |

| **WHAUL medium, pH 7.0** | **Conc.** |
|---|---|
| WHAUL powder | 1.1 g |
| | Milli-Q water 850 mL |
| Sterilize by autoclaving | |
| Supplemented with | |
| YNB 10X | 10%v/v |
| 40% glucose | 5%v/v |

| **WHAUL agar, pH 7.0** | **Conc.** |
|---|---|
| WHAUL powder | 1.1 g |
| Bacto agar | 20 g |
| | Milli-Q water 850 mL |
| Sterilize by autoclaving | |
| Supplemented with | |
| Histidine 100X | 10% v/v |
| YNB 10X | 10% v/v |
| 40% glucose | 5% v/v |

| **FDGlu assay medium, pH 7.0** | **Conc.** |
|---|---|
| BU salts 10X | 10%v/v |
| FDGlu | 10 µM |
| 3-AT | 2 mM |
| | add WHAUL medium |

| **YPD medium** | **Conc.** |
|---|---|
| Bacto peptone | 2% m/v |
| Bacto yeast extract | 1% m/v |
| dextrose | 2% m/v |
| | add Milli-Q water |
| Sterilize by autoclaving | |

| **YPD agar** | **Conc.** |
|---|---|
| Bacto peptone | 2% m/v |

| | |
|---|---|
| Bacto yeast extract | 1% m/v |
| dextrose | 2% m/v |
| Bacto agar | 2% m/v |
| | add Milli-Q water |

Sterilize by autoclaving

### 3.1.8 Primers

Primers for mutagenesis experiments were designed with the NEBaseChanger™ software online. All primers were provided by Biolegio (the Netherlands). Primers used to generate the constructs are listed in Table 1, primers for subcloning in Table 2, primers for sequencing in Table 3 and primers for quantitative Real Time-PCR (qRT-PCR) in Table 4.

| **Constructs name** | **5'- to -3'** |
|---|---|
| $ET_AR$ ECL1 Ala | F: tgccgctgccgctgccGTATTTCTTTGCAAGCTGTTC<br>R: gcagcagccgcggccgcAGCCAGCAGCTTAAATAC |
| $ET_AR$ ECL3 Ala | F: gcggccgcagctgcagcagctAGTTTCTTACTGCTCATGG<br>R: ggccgctgcggcagccgcagcTTTCTTCAATATACGGCTTAAG |
| $ET_AR$ with ECL2 of $AT_1R$ | F: TACAGTTTGTGCTTTCCATTATGAGTCCCAAAATTCAACCCTCCCGGATGTAAAGGACTGGTGGCTCTTCG<br>R: ATATTGGTGTTCTCAATGAAAAATACATTTCGATGGATCGCTTCAGGAATGGCCAG |

Table 1. Primers for constructs generation

| **Sub-cloning primer** | **5'- to -3'** |
|---|---|
| $ET_AR$ pcDNA3 | F: AGGGAGACCCAAGCTTATGGAAACCCTTTGCCTCA<br>R: TAGATGCATGCTCGAGTCAGTTCATGCTGTCCTTAT |

Table 2. Primer for subcloning

| Sequencing primers | 5'- to -3' |
|---|---|
| p426GPD (from nucleotides 4025 to 4046) | Forward: TTGACCCACGCATGTATCTATC |
| pcDNA cmv (from nucleotides from 769 to 789) | Forward: CGCAAATGGGCGGTAGGCGTG |
| $ET_AR$ (from nucleotides 446 to 465) | Forward: ATCACAATGACTTTGGCGTA |
| $ET_AR$ (from nucleotides 715 to 734) | Forward: TGTATGCTCAATGCCACATC |

Table 3. Primers for sequencing

| Primers for qRT-PCR | Sequence |
|---|---|
| Human EDNRA se | gATAgCCAgTCTTgCCCTTg |
| Human EDNRA ase | CAgAggTTgAggACggTgAT |
| Yeast GAPDH se | AGACTGTTGACGGTCCATCC |
| Yeast GAPDH ase | CAACAGCGTCTTCGGTGTAA |

Table 4. Primers for quantitative Real Time-PCR

## 3.2 Methods

### 3.2.1 Generation of constructs

#### 3.2.1.1 Preparation of the linearized vector by restriction enzyme digestion

One μg of the plasmid was linearized using two appropriate restriction enzymes in the requested digestion buffer in a 50 μL reaction. Samples were incubated at 37°C for three hours and digestion was verified on an agarose gel.

#### 3.2.1.2 Agarose gel electrophoresis

0.9% agarose gel was prepared in 1X TBE. 5μL of Midori Green was added to every 100mL of gel. The solid gel was placed into a gel electrophoresis apparatus filled with 1X TBE. Samples were mixed with 6X agarose gel loading buffer to 1X final. DNA marker (1 kb DNA ladder) was run together with the samples as a molecular weight indicator. Samples were migrated at 100 V for 45 minutes and examined under ultraviolet light at 302 nm using an UV-transilluminator.

#### 3.2.1.3 Purification of digested vector

The digested plasmid was purified with a PeqGOLD MicroSpin Cycle-pure kit according to the manufacturer's instructions. After purification, the vector was free of enzymes and ready to be directly used for ligation. The concentration was measured using a NanoDrop® Spectrophotometer.

#### 3.2.1.4 PCR amplification of target fragment

To subclone a PCR product into the digested plasmid, In-Fusion cloning kit was used according to the manufacturer's instructions. Amplification of the DNA target was performed with CloneAmp HiFi PCR Premix, which contains dNTPs and optimized buffer, allowing rapid set-up of PCR reactions. The PCR reaction components are listed in Table 5 and the reaction conditions are shown in Table 6. PCR primers were designed for the target gene with 5' 15-bp extensions that are homologous to the ends of the linearized vector (Table 2). The PCR product was verified on an agarose gel.

| **Reagent** | **Volume/Quantity** | **Final conc.** |
|---|---|---|
| CloneAmp HiFi PCR Premix | 12.5µL | 1X |
| 10 µM Forward Primer | 5 pmol | 0.2 µM |
| 10 µM Reverse Primer | 5 pmol | 0.2 µM |
| Template | < 100 ng | 20 ng |
| Sterilized distilled water | up to 25 µL | |

Table 5. Master Mix components

| **Temperature** | **Time** | **Amplification cycle** |
|---|---|---|
| 98°C | 10 sec | |
| 60°C | 15 sec | X 35 cycles |
| 72°C | 30 sec | |

Table 6. Reaction conditions

#### 3.2.1.5 Set up of In-Fusion cloning reaction

The In-Fusion HD Cloning kit enables fast, directional cloning of one fragment of DNA into any vector. The PCR product generated in the previous step was first treated with the Cloning Enhancer in order to be purified. The In-Fusion Enzyme was then used to fuse the DNA fragment and the linearized vectors effectively and precisely by recognizing 15-bp overlaps at their ends. The reaction components are listed in Table 7 and the procedures were performed according to manufacturer's instructions.

| **Component** | **Volume** |
|---|---|
| 5X In-Fusion HD Enzyme Premix | 2 µL |
| Linearized Vector | 1µL |
| Cloning Enhancer Treated PCR Insert | 1µL |
| $dH_2O$ | 6 µL |

Table 7. In-Fusion cloning reaction

#### 3.2.1.6 Bacterial transformation

Foreign DNA can be introduced into bacteria by transformation; this enables plasmid amplification and an easy collection. By exposing competent cells to a 42°C heat shock, a pressure difference between the outside and the inside of the cell is created. This leads to the formation of pores in the membrane, through which supercoiled plasmid DNA can easily enter. Followed by incubation on ice, the cell wall is closed and the plasmids are kept inside. Stellar™ Competent Cells (Table 8) were used for the transformation. 2.5 µL of the cloning product was added to 50 µL of bacteria and the transformation steps were performed according to the manufacturer's instructions. The vectors employed contained an ampicillin resistant gene, conferring antibiotic resistance to all bacteria containing the plasmid, allowing them to grow on ampicillin plates (100 µg/mL). Plates were incubated at 37°C overnight.

| Bacteria | Provider | Genotype |
|---|---|---|
| Stellar™Competent Cells | Takara | *F-, endA1, supE44, thi-1, recA1, relA1, gyrA96, phoA, Φ80d lacZ Δ M15, Δ(lacZYA-argF) U169, Δ(mrr-hsdRMS-mcrBC), Δ mcrA, λ-* |

Table 8. Bacteria genotype

#### 3.2.1.7 Mini-prep

A pre-culture of LB medium containing 100 µg/mL ampicillin was inoculated with a single colony picked from the LB-Ampicillin agar plate containing the bacteria transformants. 3 mL of the pre-culture was centrifuged at room temperature. All steps were carried out according to the GeneJET Plasmid Miniprep Kit protocol. The nucleic acid concentration was measured by NanoDrop® Spectrophotometer. The plasmids were stored at -20°C.

#### 3.2.1.8 Screening for positive plasmids

Plasmids isolated by mini-prep were digested by the two restriction enzymes used to linearize the vector in a 25 µL reaction. Samples were incubated at 37°C for three hours and then run on an agarose gel. Plasmids showing two bands corresponding to the molecular size of the vector and the insert were considered positive.

#### 3.2.1.9 DNA sequencing and alignment

The plasmids potentially containing the insert were sequenced by the company LGC Genomics GmbH using appropriate primers (Table 3). The resulting sequences were analyzed by using the DNASTAR MegAlign 14 software.

#### 3.2.1.10 Midi-prep

The NucleoBond® Xtra Midi/Maxi and Endotoxin Free (EF) kits were used to extract a large amount of plasmid DNA for mammalian cell and yeast experiments. After sequencing, one single positive colony was incubated in LB medium with 100 µg/mL ampicillin for eight hours. This pre-culture was then diluted 1 to 1000 into 100 mL LB medium containing 100 µg/mL ampicillin and

incubated overnight at 37°C under shaking. The High-copy protocol was performed according to manufacturer's instructions. After elution and precipitation, plasmid DNA was dissolved in Tris buffer. The nucleic acid concentration was measured by NanoDrop® Spectrophotometer. The plasmids were stored at -20°C for further use.

#### 3.2.1.11 Bacterial glycerol stock

Glycerol stocks enable long-term storage of bacteria. A pre-culture of LB medium containing 100 µg/mL ampicillin was inoculated with the colony to be preserved and shaken six hours at 37°C. 250 µL of the pre-culture was added to 750 µL of 60% glycerol and gently mixed. Then the glycerol stock was frozen at -80°C.

### 3.2.2 Generation of mutated constructs

#### 3.2.2.1 Site-directed mutagenesis

Mutated constructs were generated using the Q5® Site-Directed Mutagenesis Kit according to the manufacturer's instructions. Briefly, exponential amplification of cDNA fragment encoding $ET_AR$ was performed with Q5 Hot Start High-Fidelity DNA Polymerase along with specific primers designed using NEBaseChanger (Table 1). The forward primer was designed to incorporate the desired nucleotide change in its center, and also to include at least 10 complementary nucleotides on the 3' side of the mutation. The reverse primer was designed to anneal back to back at the 5' ends of the two primers. The experimental conditions of PCR are listed in Tables 9, 10 and 11. The PCR products were then treated with the Kinase-Ligase-*Dpnl* (KLD) enzyme, which enables a quick circularization and template removal at room temperature (Table 12). Transformation into high-efficiency NEB 5-alpha-Competent E. *coli* ensures high numbers of transformants on LB-Ampicillin plates. The transformation was performed using NEB 5-alpha-Competent *E.coli* (Table 13). The procedure was the same as described in 2.2.1.6.

| **Component** | **25**µL RXN | **Final conc.** |
|---|---|---|
| Q5 Hot Start High-Fidelity 2X Master Mix | 12.5µL | 1X |
| 10 µM Forward Primer | 1.25µL | 0.5 µM |

| **Component** | **25**µL RXN | **Final conc.** |
|---|---|---|
| 10 µM Reverse Primer | 1.25µL | 0.5 µM |
| Template DNA | 1µL | 1-25 ng |
| Nuclease-free water | 9.0µL | |

Table 9. Reaction components

| **Construct** | **DNA template** | **DNA quantity** |
|---|---|---|
| $ET_AR$ ECL1 Ala | p426 GPD $ET_AR$ wild type plasmid | 10 ng |
| $ET_AR$ ECL3 Ala | p426 GPD $ET_AR$ wild type plasmid | 10 ng |
| $ET_AR$ with ECL2 of $AT_1R$ | p426 GPD $ET_AR$ wild type plasmid | 10 ng |

Table 10. Components of PCR reactions for the different constructs

| **Construct** | **Second denaturation** | **Annealing** | **Elongation step** |
|---|---|---|---|
| $ET_AR$ ECL1 Ala | 98°C 10 s | 67.6°C 30 s | 72°C 6min |
| $ET_AR$ ECL3 Ala | 98°C 10 s | 60°C 30 s | 72°C 6min |
| $ET_AR$ with ECL2 of $AT_1R$ | 98°C 10 s | 70°C 30 s | 72°C 4min |

Table 11. PCR conditions for the different constructs

| **Components** | **Volume** | **Final conc.** |
|---|---|---|
| PCR Product | 1 µL | |
| 2X KLD Reaction Buffer | 5 µL | 1X |
| 10X KLD Enzyme Mix | 1 µL | 1X |
| Nuclease-free Water | 3 µL | |

Table 12. KLD treatment components

| **Bacteria** | **Provider** | **Genotype** |
|---|---|---|
| NEB 5-alpha Compent *E.coli* | NEB | *fhuA2, Δ(argF-lacZ) U169, phoA, glnV44, Φ80 Δ(lacZ)M15, gyrA96, recA1, relA1, endA1, thi-1, hsdR17* |

Table 13. Bacteria genotype

After transformation, clones were amplified and sequenced as described in 2.2.1.7 to 9. A midi-prep was performed to produce appropriate quantities of the plasmids as described in 2.2.1.10.

### 3.2.3 Patient IgG isolation

The isolation of immunoglobulins class G (IgG) was carried out from plasma of patients suffering from systemic sclerosis. These patients were tested positive for the presence of antibodies targeting $ET_AR$ ($ET_AR$-IgG). Plasma was filtered through 0.45 µm filters before use. HiTrap Protein G HP columns packed with Protein G Sepharose™ High Performance, which can strongly bind to the Fc region of IgG were used for the isolation. After the plasma was diluted 1:2 with binding buffer run through the column, the $ET_AR$-IgG solution was eluted, neutralized and dialyzed against WHAUL medium or DMEM low glucose, depending on whether the stimulation was performed on yeasts or mammalian cells. After dialysis, aliquots of the IgG were sent to Labor Berlin and the concentrations were measured by ELISA.

### 3.2.4 GPCR activation assay in yeast

The yeast GPCR activation assay in yeast is well-established as an experimental system for the detection of receptor activation [49] [50] [51]. Mating in haploid yeast cells is stimulated by pheromone binding to GPCRs. The MMY yeast strains provided by the GlaxoSmithKline Company were modified to express chimeric G-proteins, in which the five C-terminal residues of Gpa1p were replaced by the corresponding sequence of the human $G_\alpha$ subunits (Table 14). Furthermore, these yeasts do not express the yeast GPCR anymore but depend on the expression of a human GPCR, able to bind to the yeast chimeric G-protein in order to grow.

| **Strain** | **Genotype** |
|---|---|
| MMY11 | *MAT***a** *his3 leu2 trp1 ura3 can1 gpa1*Δ*::ADE2 far1*Δ*::ura3 sst2*Δ*::ura3*Δ *fus1::FUS1-HIS3 LEU2::FUS1-lacZ ste2*Δ*::G418$^R$* [49] |
| MMY14 | MMY11 *TRP1::Gpa1/$G_\alpha^{q(5)}$* [51] |

Table 14. Genotypes of yeast strains used for GPCR activation assay

#### 3.2.4.1 Yeast transformation

The procedures are similar to the ones described by Dr. med. Nan Zhu in her thesis [Development of a molecular toolbox to study the cross-talk between Angiotensin II type 1 and Endothelin-1 type

A receptors in the context of obliterative vasculopathy, http://www.diss.fu-berlin.de/diss/receive/FUDISS_thesis_000000100230]. Briefly, yeasts were recovered from -80 °C and spread on a YPD plate. A single colony was put into YPD medium and incubated overnight at 30°C, as a pre-culture. On the next day, 100mL of YPD medium was inoculated and the yeasts were harvested after two to three hours. Transformation was performed using the lithium acetate (LiAc)/ single-stranded DNA (ssDNA)/ polyethylene glycol (PEG) method. Transformed yeast cells were plated on WHAUL-His plates and incubated for three or four days.

#### 3.2.4.2 Measuring gene expression in yeast

Yeast transformation with different amounts of plasmid was performed. Colonies were picked after three or four days and incubated in 3 mL YPD medium at 30°C overnight under shaking. Yeast samples were obtained on the next day by centrifugation. The total RNA was extracted using Direct-zol™ RNA MiniPrep, which can provide a streamlined method for purification of up to 100 µg per prep of high-quality RNA directly from samples. The RNA concentration was measured by NanoDrop® Spectrophotometer. Reverse Transcription (RT)-PCR was performed to obtain cDNA, the RT-PCR components are shown in Table 15. Quantitative Real Time-PCR (qRT-PCR) using Applied Biosystems® 7500 qRT-PCR System was performed, components are shown in Table 16. The amount of fluorescence released during amplification cycle is proportional to the relative quantity of mRNA initially present.

| **Content** | **Volume (1X) / Amount** |
|---|---|
| 10X M-MuLV Reverse transcriptase Buffer | 5µL |
| dNTP mix 10 mM | 8µL |
| RNase inhibitor | 1µL |
| M-MuLV Reverse transcriptase 200,000U/mL | 0.25µL |
| Oligo | 1µL |
| RNA | 500ng |
| Total | 50µL |

Table15. RT-PCR system

| Content | Volume (1X) |
|---|---|
| SYBR Green | 4µL |
| Primer se 10 µM | 0.5µL |
| Primer ase 10 µM | 0.5µL |
| ddH2O | 7µL |
| cDNA | 1µL |
| Total | 13µL |

Table16. qRT-PCR system

#### 3.2.4.3 Yeast GPCR assay

Four days after transformation, four clones from transformed yeasts were picked-up and transferred individually into WHAUL medium containing Histidine and incubated overnight at 30°C under shaking. Each pre-cultured clone was then added to FDGlu assay medium (lacking Histidine) containing different concentrations of $ET_AR$-IgG (0, 0.5, 1.0 and 1.5 mg/mL) in 96-well plates. 3-AT in the FDGlu assay medium is a competitive inhibitor of the *HIS3* enzyme which can regulate background activity caused by leakiness of the reporter or constitutive activity of the GPCR. Plates were protected from light and incubated at 30°C under shaking. After incubation for 16 hours, fluorescent measurement was performed at an excitation of 485 nm and emission of 535 nm.

### 3.2.5 Luciferase reporter assay

Activation of $G_{q/11}$ or $G_{12/13}$ can be monitored with the binding of specific transcription factors, NFAT and SRF to the luciferase promoter.

#### 3.2.5.1 Human microvascular endothelial cells (HMEC-1)

HMEC-1 cells were grown in flasks with complete growth medium in a humidified atmosphere with 5% $CO_2$ at 37 °C. T75 flasks and 24 wells plates were pre-coated with 0.2% gelatin. The cells

were passaged at 90 % confluence and used to seed 24 wells plates for the experiments. Cells were briefly washed once with PBS, then deattached with 1X Trypsin added into the flask for five minutes. Complete medium was used to deactivate the enzyme. After centrifugation and resuspension in complete medium, the cells were counted with a Neubauer cell chamber in the presence of Trypan blue to assess their viability. To further cultivate the cells, 1.5 million cells were seeded into a T75 flask. For experimental purposes, 50,000 cells per well were added into each well of the 24-well coated plates.

#### 3.2.5.2 Transient transfection

After seeding, the cells were allowed to grow for four days before the transfection was performed. HMEC-1 cells were transfected transiently with 250 ng of two plasmids, a pcDNA3 plasmid enabling the expression of the wild-type or mutated $ET_A$ receptor and a plasmid containing a reporter specific to NFAT or SRF. Transfection was performed in starvation medium using the Xfect™ Transfection Reagent following the manufacturer's instructions. 16 hours later, medium was changed to complete medium.

#### 3.2.5.3 Cell stimulation

To study the functionality of the receptors, ET-1 and $ET_A$R-IgG were used to stimulate the transfected cells. 48 hours after transfection, the medium was changed to starvation medium. One hour later, cells were treated with ET-1 (100 nM) or $ET_A$R-IgG (1.0 mg/mL) or DMEM Low Glucose as controls.

#### 3.2.5.4 Luciferase measurement

After six hours of stimulation, cells were washed once in PBS and lysed with 1X PLB for 15 minutes under shaking. Luciferase quantity was assessed with the Luciferase Reporter Kit according to the manufacturer's instructions and measured in a FLUOstar microplate reader using the OPTIMA software.

### 3.2.6 Statistical analysis

Data are expressed as mean ± SEM, *n* stands for the number of independent experiments. Comparison between wild type non-stimulated and other groups were analyzed by Wilcoxon test; the other comparisons were performed by Mann-Whitney U test. Differences were considered significant when one-tailed tests *p* value was smaller than 0.05. GraphPad Prism software version 5.01 was used for the calculations.

# 4 Results

## 4.1 Generation of human Endothelin-1 type A receptor mutants

The extracellular loops (ECL) of $ET_AR$ are potential binding sites for patients' antibodies, thus mutants of the ECL regions of $ET_AR$ to Alanine were generated to test their involvement in the receptor immune activation.

### 4.1.1 Generation of yeast expressing $ET_A$ wild-type and mutant receptor

The p426 GPD plasmid allows the expression of a gene of interest in yeasts. The ampicillin resistance gene expressed by the plasmid enables selection in *E. coli* (Figure 4). Three constructs had been previously generated in the p426 GPD plasmid in the lab: the human wild-type $ET_AR$ ($ET_AR$ WT), a mutant in which the first ECL of human $ET_AR$ was substituted for Alanine ($ET_AR$ ECL1 Ala) and a mutant where $ET_AR$ second ECL was replaced by the second ECL of $AT_1R$ ($ET_AR$ with ECL2 of $AT_1R$, [Development of a molecular toolbox to study the cross-talk between Angiotensin II type 1 and Endothelin-1 type A receptors in the context of obliterative vasculopathy, http://www.diss.fu-berlin.de/diss/receive/FUDISS_thesis_000000100230]).

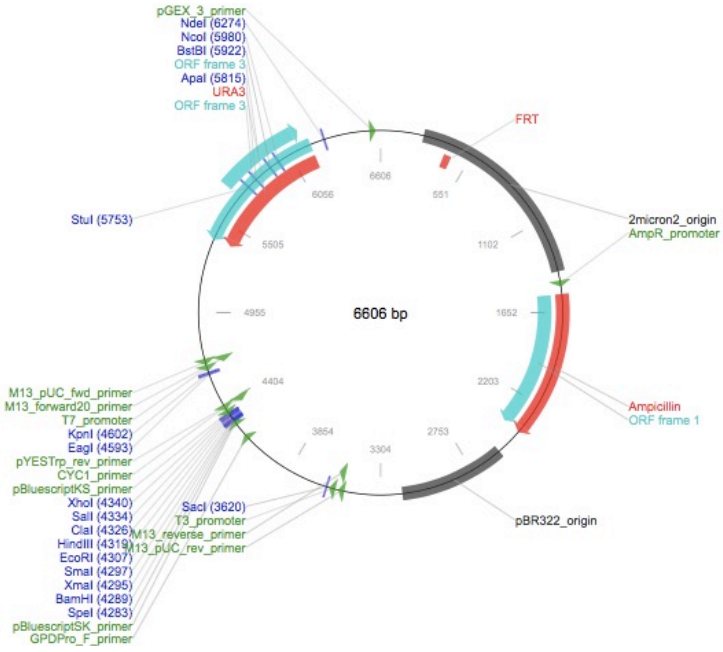


Figure 4. Map of p426 GPD (6606 base pairs).

In order to mutate the third extracellular loop of $ET_AR$ to Alanine, a site-directed mutagenesis was realized. PCR amplification was performed using the p426 GPD $ET_AR$ WT construct as template and primers were specially designed for site-directed mutagenesis (Table 1). After transformation, the plasmid was purified and DNA was sequenced. As shown in figure 5, the third ECL of $ET_AR$ was correctly substituted to Alanine.

A

$ET_AR$ WT ECL3 ACTGTGTATAACGAGATGGACAAGAACCGATGTGAATTACTT

$ET_AR$ ECL3 Ala GCTGCGGCTGCCGCAGCGGCCGCGGCCGCAGCTGCAGCAGCT

B

$ET_AR$ WT ECL3 TVYNEMDKNRCELL

$ET_AR$ ECL3 Ala AAAAAAAAAAAAAA

Figure 5. Mutation of $ET_AR$ ECL3 to Alanine. (A) DNA Sequence of the third ECL of $ET_AR$ wild type and mutant. (B) Amino acid translation of the sequences. Mismatches are shown in red.

### 4.1.2 Generation of mammalian cells expressing $ET_A$ wild-type and mutant receptor

The pcDNA3 plasmid (Figure 6) was used to express the human Endothelin-1 type A receptor in mammalian cells. The ampicillin resistance gene in the plasmid allows selection in *E. coli*.

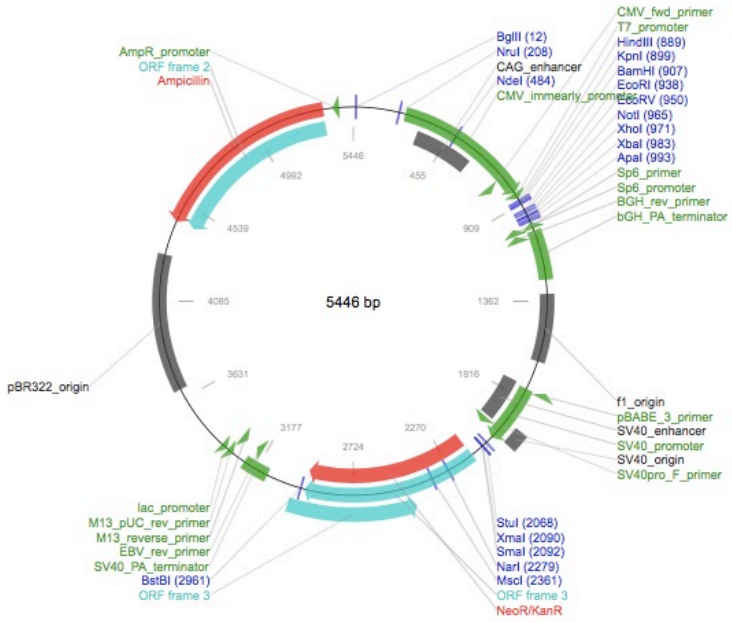


Figure 6. Map of the pcDNA3 plasmid (5446 base pairs).

*Hind*III and *Xho*I restriction enzymes were used to linearize the plasmid. PCR primers were designed with 5' 15-bp extensions homologous to the ends of the linearized vector and p426 GPD $ET_AR$ constructs were used as templates. The appropriate insert and the linearized plasmid were ligated and transformed into *E. coli*.

#### 4.1.2.1 Generation of pcDNA3 $ET_AR$ WT

Digestion of pcDNA3 $ET_AR$ WT with the two cloning enzymes, *Hind*III and *Xho*I, should produce three fragments, one 82 base pair (bp)-long fragment and one 5364 bp-long corresponding to the pcDNA3 plasmid, one 1281 bp-long fragment corresponding to human $ET_AR$. Figure 7 shows plasmids of ten ampicillin resistant colonies obtained after cloning. All plasmids showing two bands of the right size were considered positive as the 82 bp-long fragment was too small to be detected.

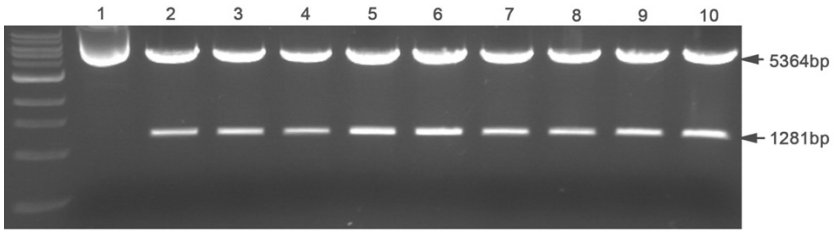


Figure 7. Double digestion of ten ampicillin-resistant colonies. Plasmids 2 to 10 are positive.

In order to verify the absence of mutations, the positive plasmids were sequenced and aligned with the sequence of the template. Two positive plasmids without any mutations were chosen to perform the luciferase reporter assays.

#### 4.1.2.2 Generation of pcDNA3 $ET_AR$ ECL1 Ala

The p426 GPD $ET_AR$ ECL1 Ala construct was used as template to sub-clone the $ET_AR$ ECL1 Ala fragment to pcDNA3. Six colonies obtained after transformation were picked and verified by double digestion, as done for wild type $ET_AR$. All colonies showed two bands, corresponding respectively to the linearized pcDNA3 plasmid and the insert (Figure 8). One clone was completely sequenced (Figure 9) and was used in further cell experiments.

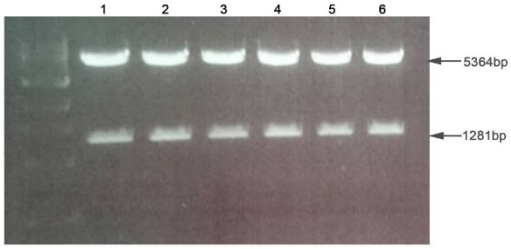


Figure 8. Double digestion of plasmids from colonies potentially containing the pcDNA3 $ET_AR$ ECL1 Ala plasmid.

A

$ET_AR$ WT ECL1 GGGCGCTGGCCTTTTGATCACAATGACTTTGGC

$ET_AR$ ECL1 Ala GCGGCCGCGGCTGCTGCTGCCGCTGCCGCTGCC

B

$ET_AR$ WT ECL1 GRWPFDHNDFG

$ET_AR$ ECL1 Ala AAAAAAAAAAA

Figure 9. Mutation of $ET_AR$ ECL1 to Alanine. (A) Sequence of the first ECL of $ET_AR$ wild type and mutant. (B) Amino acid translation of the sequences. Mismatches are shown in red.

### 4.1.2.3 Generation of pcDNA3 $ET_AR$ with ECL2 of $AT_1R$ and pcDNA3 $ET_AR$ ECL3 Ala

These sub-cloning experiments were made using the same protocol as that used for the ECL1 mutant. In each case, from the positive plasmids found after double digestion, one was completely sequenced (Figure 10 and 11) and used for luciferase assays if it was free of mutations.

A

$ET_AR$ WT ECL2 ATTGGCTTCGTCATGGTACCCTTTGAATATAGGGGTGAACAGCATAAAACCTGTATGCTCAATGCCACATCAAAATTCATGGAGTTCTACCAA

$ET_AR$ with ECL2 of $AT_1R$ ATCCATCGAAATGTATTTTTCATTGAGAACACCAATATTACAGTTTGTGCTTTCCATTATGAGTCCCAAAATTCAACCCTCCCG

B

$ET_AR$ WT ECL2 IGFVMVPFEYRGEQHKTCMLNATSKFMEFYQ

$ET_AR$ with ECL2 of $AT_1R$ IHRNVFFIENTNITVCAFHYESQNSTLP

Figure 10. Mutation of $ET_AR$ with ECL2 of $AT_1R$. (A) Sequence of the second ECL of $ET_AR$ and $AT_1R$ wild type. (B) Amino acid translation of the sequences.

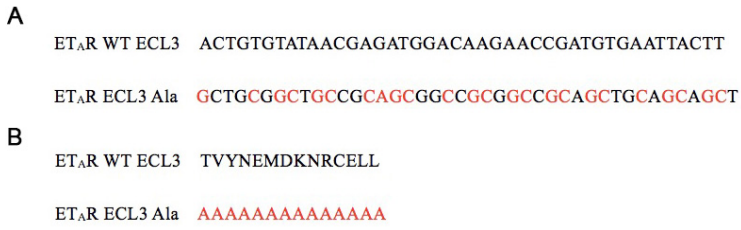


Figure 11. Mutation of $ET_AR$ ECL3 to Alanine. (A) DNA Sequence of the third ECL of $ET_AR$ wild type and mutant. (B) Amino acid translation of the sequences. Mismatches are shown in red.

## 4.2 Effects of the structure of the extracellular loops on $ET_AR$ activation

In order to study the influence of the structure of each extracellular loop on $ET_AR$ activation, a GPCR activation assay already established for previous yeast batches in the lab was applied [Development of a molecular toolbox to study the cross-talk between Angiotensin II type 1 and Endothelin-1 type A receptors in the context of obliterative vasculopathy, http://www.diss.fu-berlin.de/diss/receive/FUDISS_ thesis_000000100230]. This assay had to be first optimized for novel experimental conditions.

### 4.2.1 Optimization of the GPCR activation assay

In the MMY yeast model, the yeast's growth depends on the activation of the expressed human GPCR. Dependent on the kind of receptor transformed, several parameters had to be optimized.

#### 4.2.1.1 Optimization of MMY yeast transformation

The first step was to improve MMY yeast transformation, first, by determining the optimal plasmid amount. Total RNA extracted from transformed or non-transformed yeast cells was subjected to RT-PCR to obtain cDNA. Then, quantitative RT-PCR was performed to determine the human $ET_AR$ wild-type expression level. After normalization to yeast GAPDH, the $ET_AR$ expression level was calculated as relative to control (non-transformed yeasts). Results showed that transformation

with 0.5-µg plasmid achieved the lowest expression, 3-µg the best (Figure 12A). Then, optimal incubation times after transformation were investigated to obtain high $ET_AR$ transcription levels. As shown in figure 12B, yeasts transformed with 1-µg plasmid and incubated for four days had the highest receptor expression level. Therefore, this condition was used in further experiments.

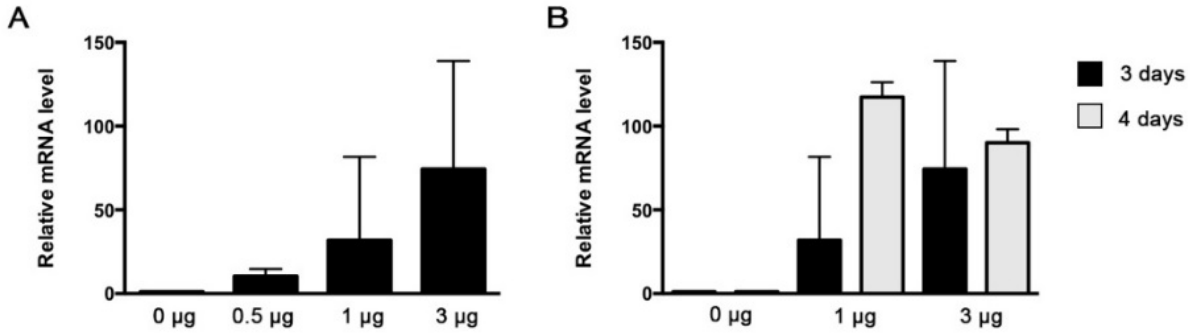


Figure 12. $ET_AR$ wild-type transcription level in yeast (A) Yeasts were transformed with different amounts of plasmid and incubated for three days. (B) Yeasts were transformed with different amounts of plasmid and incubated for three or four days after transformation. Values are from three colonies and presented as mean ± SD.

#### 4.2.1.2 Optimization of the GPCR assay

Three parameters were further modulated to optimize the GPCR assay: the first is 3-AT (3-amino triazole), which is a competitive inhibitor of the *HIS3* protein moderating background yeast growth caused by leakiness of the receptor or constitutive activity of the GPCR [51]. The second, the way to inoculate the yeast cultures before the assay and the third parameter is the seeding density of the yeast cells into the assay medium, which can also influence the outcome of the assay. All three parameters were tested but only the way of inoculation of the yeast cultures showed effects.

For the first inoculation method, single colonies were picked with a sterile toothpick 72 hours after transformation, streaked onto a WHAUL+His plate for further 24 hours and then scraped and inoculated into 200 µL of WHAUL+His medium. For the second method, transformed yeast clones were picked after four days and single colonies were directly inoculated into 100 µL of WHAUL+His. In each case, yeast cells grown overnight in WHAUL+His were stimulated with ET-1 in increasing concentrations: 0, $10^{-7}$, $5*10^{-7}$ and $10^{-6}$ M. As shown in figure 13, the second

inoculation way gave the strongest fluorescence intensity and showed a dose-dependent activation of $ET_AR$ upon stimulation with ET-1.

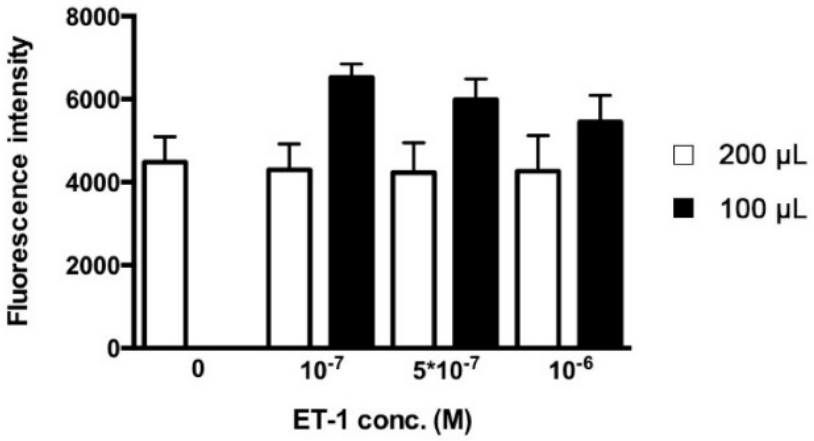


Figure 13. Yeast growth after ET-1 stimulation. Two methods of inoculation were compared. Yeast growth is reflected by the fluorescence intensity. Ten wells of a single colony were measured and the data are presented as mean ± SD.

### 4.2.2 $ET_AR$ activation by $ET_AR$-IgG and involvement of the extracellular loops

MMY14 strain expressing $G_{q/11}$ was transformed with p426GPD $ET_AR$ WT or mutant. In this model, it has already been shown that ET-1 activates $ET_AR$ dose-dependently [Development of a molecular toolbox to study the cross-talk between Angiotensin II type 1 and Endothelin-1 type A receptors in the context of obliterative vasculopathy, http://www.diss.fu-berlin.de/diss/receive/FUDISS_thesis_000000100230]. Therefore, the focus was on the IgG-mediated activation of the receptor. Yeasts were stimulated with increasing concentrations of $ET_AR$-IgG (0, 0.5, 1 and 1.5 mg/mL) isolated from systemic sclerosis (SSc) patients tested positive for $ET_AR$-IgG in ELISA. After 16 hours of incubation, fluorescence intensity was measured.

#### 4.2.2.1 $ET_AR$-IgG activate the wild-type receptor

When the yeast cells were stimulated with $ET_AR$-IgG after transformation with the wild-type

receptor, the yeast growth increased significantly when comparing stimulated yeasts to non-stimulated yeasts (Figure 14). Therefore, IgG isolated from patients was able to induce activation of the receptor.

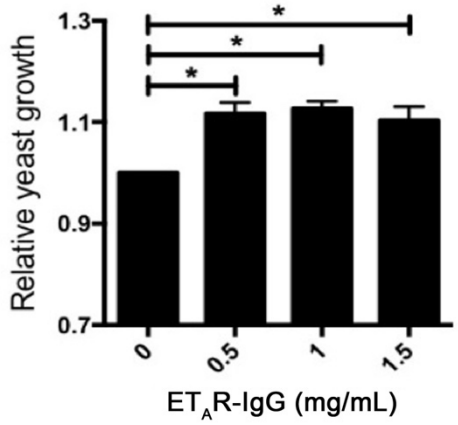


Figure 14. MMY 14 $ET_AR$ wild-type yeast growth in GPCR activation model stimulated with $ET_AR$-IgG. Yeast growth is depicted as relative to yeast growth without stimulation. Data are from six experiments and presented as mean ± SEM, * $p < 0.05$.

#### 4.2.2.2 Involvement of the extracellular loops in $ET_AR$ activation

##### 4.2.2.2.1 The second extracellular loop is not involved in $ET_AR$ activation

A thesis done in the laboratory had already shown that the second extracellular loop was not necessary for the receptor activation [Development of a molecular toolbox to study the cross-talk between Angiotensin II type 1 and Endothelin-1 type A receptors in the context of obliterative vasculopathy, http://www.diss.fu-berlin.de/diss/receive/FUDISS_thesis_000000100230]. Hence, the focus of this study was on the first and third loops.

##### 4.2.2.2.2 The first extracellular loop is involved in $ET_AR$ activation

Yeast expressing the receptor mutated in the first ECL showed a trend to a higher growth rate even without antibodies stimulation. Increasing the concentrations of the stimuli did not bring any further activation in yeasts expressing the mutant receptor (Figure 15), suggesting that there could be a constitutive activation of the receptor due to the modification of the first ECL structure.

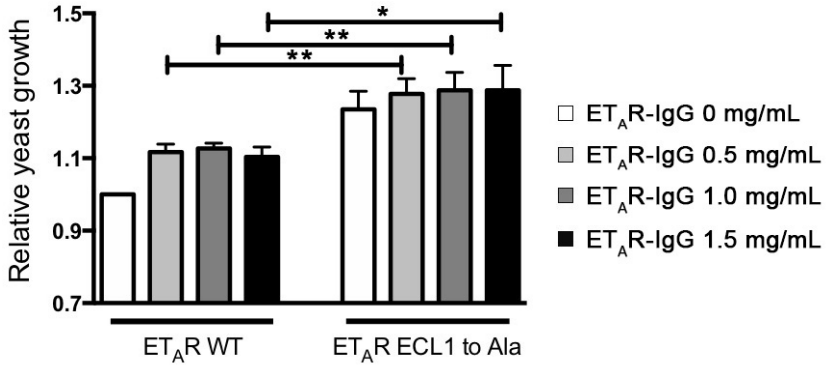


Figure 15. Yeast growth in GPCR activation model stimulated with ET$_A$R-IgG. Yeast growth is depicted relative to yeast growth without stimulation. Data are from six (WT) and four (ECL1) experiments and presented as mean ± SEM, * $p < 0.05$, ** $p < 0.01$.

#### 4.2.2.2.3 Mutating ECL3 results in ET$_A$R constitutive activation

As for the third ECL, mutation to Alanine induced a significantly stronger yeast growth already in absence of immune stimulation (Figure 16), which means that there is a constitutive activation of the mutated receptor.

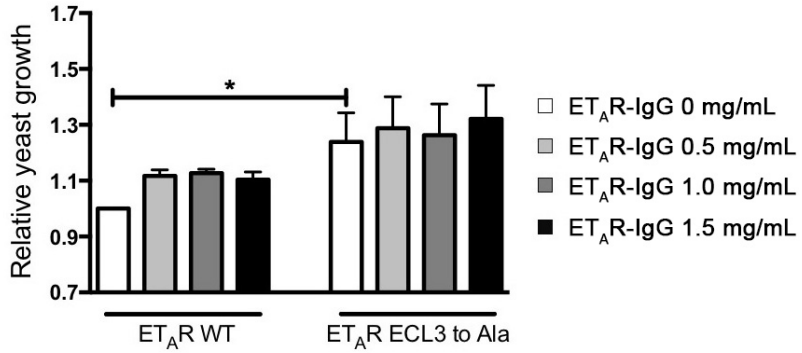


Figure 16. Yeast growth in GPCR activation model stimulated with ET$_A$R-IgG. Yeast growth is depicted relative to yeast growth without stimulation. Data are from six (WT) and seven (ECL3) experiments and presented as mean ± SEM, * $p < 0.05$.

## 4.3 Extracellular loops of $ET_AR$ trigger G-protein activation

To investigate whether structural changes affecting extracellular loops of $ET_AR$ induce the same effects in a more complex environment as in the MMY model, activation of G-proteins upon stimulation of $ET_AR$ was monitored. Human Endothelin-1 type A receptor binds to two G-proteins, $G_{q/11}$ and $G_{12/13}$, upon activation by its peptide agonist, ET-1 [9]. In order to characterize the intracellular pathways activated after receptor stimulation with IgG and to determine involvement of specific extracellular loops, the mutants used in the yeast assay were subcloned in pcDNA3 to allow their expression in mammalian cells.

$G_{q/11}$ and $G_{12/13}$ activation was monitored in luciferase reporter assays by measuring the binding of the transcription factors NFAT (Nuclear factor of activated T-cells) and SRF (Serum response factor), respectively to DNA. Human microvascular endothelial cells (HMEC-1) were transiently transfected to express either wild-type or mutated $ET_AR$ and a NFAT or SRF luciferase reporter plasmid. Cells were stimulated with the peptide agonist of the receptor, ET-1, or $ET_AR$-IgG.

### 4.3.1 G-protein activity is increased upon $ET_AR$ WT activation

In the NFAT luciferase reporter assay, cells transfected with wild-type $ET_AR$ showed a significant increase in NFAT activity in response to both ET-1 and $ET_AR$-IgG stimulation, antibodies inducing a slightly higher increase than the peptide agonist (Figure 17A). This result was concordant with those previously obtained in yeasts.

Furthermore, cells transfected with wild-type $ET_AR$ showed that ET-1 and $ET_AR$-IgG both significantly increased SRF activity. IgG-mediated activation of the receptor induced a significantly stronger activation of $G_{12/13}$ than ET-1 (Figure 17B). In conclusion, antibodies stimulating $ET_AR$ trigger a higher activation of both $G_{q/11}$ and $G_{12/13}$ than does the peptide agonist.

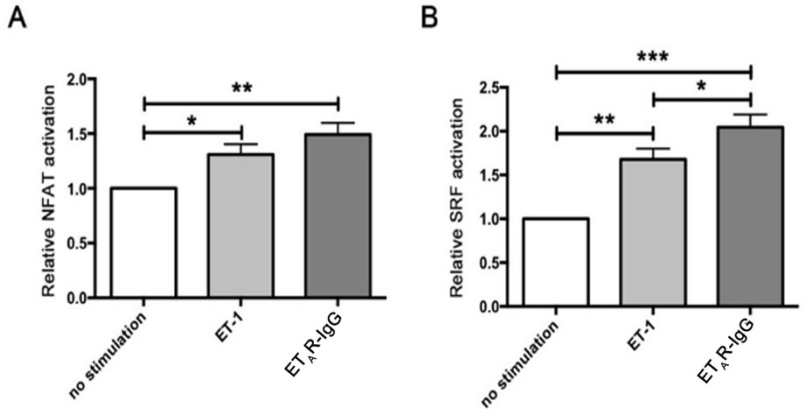


Figure 17. Relative NFAT activity (A) and SRF activity (B) in response to ET-1 and $ET_AR$-IgG stimulation in HMEC cells transfected with $ET_AR$ wild-type. NFAT or SRF activity is depicted relative to NFAT or SRF activity in absence of stimulation, respectively. Data are from nine (NFAT) and eleven (SRF) experiments and presented as mean ± SEM, * $p < 0.05$, ** $p < 0.01$, *** $p < 0.005$.

### 4.3.2 The second extracellular loop of $ET_AR$ is required for ET-1 but not for IgG-induced G-protein activation

In the yeast GPCR activation assay, replacing the second extracellular loop of $ET_AR$ by ECL2 of $AT_1R$ did not affect endogenous or IgG-mediated activation of the receptor [Development of a molecular toolbox to study the cross-talk between Angiotensin II type 1 and Endothelin-1 type A receptors in the context of obliterative vasculopathy, http://www.diss.fu-berlin.de/diss/receive/FUDISS_thesis_000000100230]. In order to verify these results in mammalian cells, this mutant was used in both NFAT and SRF luciferase reporter assay.

When the cells were transfected with pcDNA3 $ET_AR$ with ECL2 of $AT_1R$, stimulation with $ET_AR$-IgG led to significantly increased NFAT activity in comparison to non-stimulated cells (Figure 18A). Stimulation with ET-1 also showed a slight increase of NFAT activity, but it was not significant. This confirms the results observed in yeast. However, it should be noted that the $G_{q/11}$ activation upon antibodies stimulation was stronger in the mutant cells than in the wild-type cells, something that was not seen in yeasts.

In SRF luciferase reporter assay, cells that were transfected with pcDNA3 $ET_AR$ with ECL2 of

$AT_1R$ and stimulated with ET-1 showed SRF activity at non-stimulated level, revealing that intact ECL2 structure is essential for $ET_AR$ activation via its peptide agonist. Conversely, cells transfected with $ET_AR$ mutant and stimulated with $ET_AR$-IgG showed a higher activity of SRF in comparison to both non-stimulated wild-type and mutant $ET_AR$ transfected cells, even if significance was only found with wild type (Figure 18B). Hence, ECL2 does not seem necessary for antibody-triggered $ET_AR$ intracellular signaling.

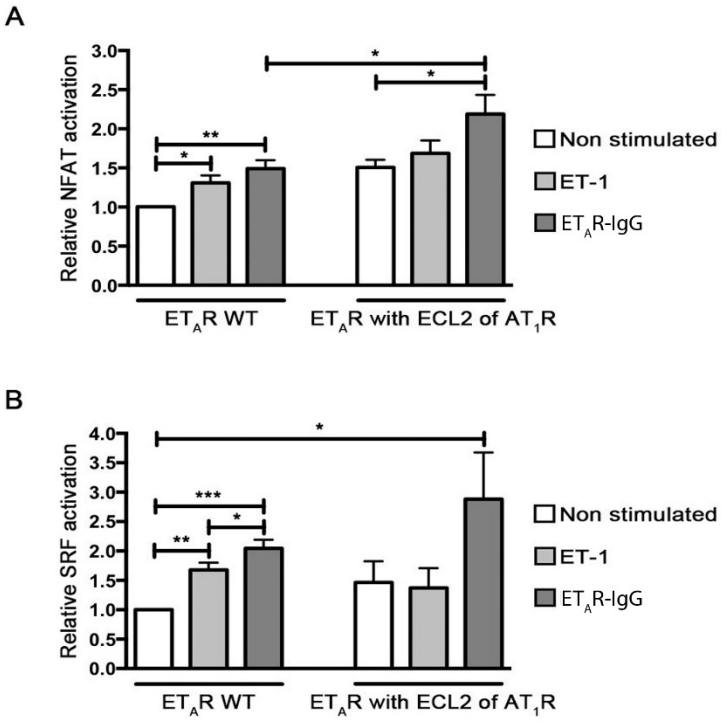


Figure 18. Relative NFAT activity (A) and SRF activity (B) in response to ET-1 and $ET_AR$-IgG stimulation in HMEC cells transfected with $ET_AR$ wild type and $ET_AR$ with $AT_1R$ ECL2. NFAT or SRF activity is depicted relative to NFAT or SRF activity in absence of stimulation, respectively. Data are from eleven (WT) and seven (ECL2) experiments and presented as mean ± SEM, * $p < 0.05$, ** $p < 0.01$, *** $p < 0.005$.

### 4.3.3 The first extracellular loop of $ET_AR$ is required for $G_{12/13}$ activation

Cells transfected with $ET_AR$ ECL1 Ala mutant and stimulated with $ET_AR$-IgG showed a significantly higher activity of NFAT in comparison to non-stimulated wild type $ET_AR$ cells. However, no constitutive activation of the receptor was observed (Figure 19A). Hence, mutation

of the receptor's first extracellular loop does not influence the activation of $G_{q/11}$ mediated by antibodies.

When the cells were transfected with $ET_AR$ ECL1 Ala and stimulated with ET-1, SRF activity stayed at non-stimulated level and was significantly decreased in comparison to the stimulation of the wild-type receptors, revealing that normal structure of ECL1 is essential for $ET_AR$-mediated $G_{12/13}$ activation via its peptide agonist. Conversely, cells transfected with $ET_AR$ ECL1 Ala and stimulated with $ET_AR$-IgG showed a significantly higher activity of SRF in comparison to non-stimulated wild type $ET_AR$ and mutant transfected cells (figure 19B). Therefore, ECL1 is not necessary for antibody-triggered $ET_AR$ intracellular signaling.

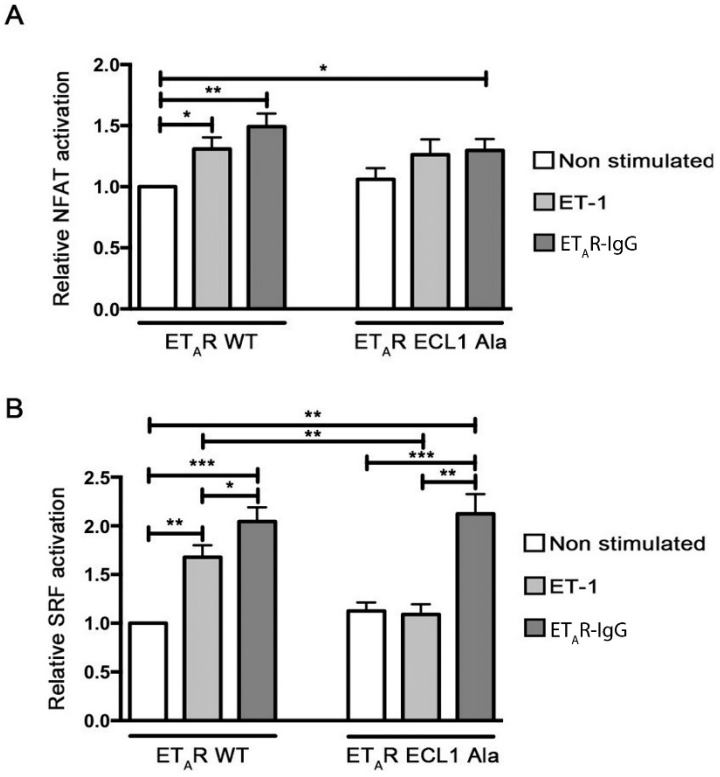


Figure 19. Relative NFAT activity (A) and SRF activity (B) in response to ET-1 and $ET_AR$-IgG stimulation in HMEC cells transfected with $ET_AR$ wild type and $ET_AR$ ECL1 Ala. NFAT or SRF activity is depicted relative to NFAT or SRF activity in absence of stimulation, respectively. Data are from eleven (WT) and eight (ECL1) experiments and presented as mean ± SEM, * $p < 0.05$, ** $p < 0.01$, *** $p < 0.005$.

### 4.3.4 Mutation of the third extracellular loop results in constitutive binding of G-proteins

When the cells were transfected with $ET_AR$ ECL3 Ala, a significant increase of NFAT activity in comparison to the wild-type $ET_AR$ transfected cells could already be seen in the absence of stimulation (figure 20A). This revealed a constitutive binding of $G_{q/11}$ to the receptor which was consistent with the results obtained in yeast experiments.

As in the NFAT study, when the cells were transfected with $ET_AR$ ECL3 Ala, a significant increase of SRF activity could be seen in the absence of stimulation, revealing a constitutive binding of $G_{12/13}$ to the mutated receptor (figure 20B).

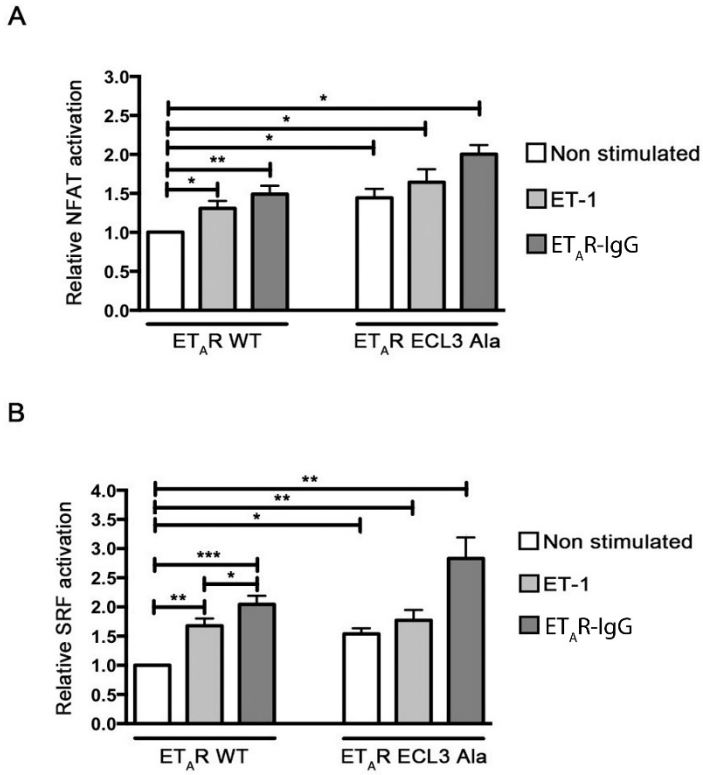


Figure 20. Relative NFAT activity (A) and SRF activity (B) in response to ET-1 and $ET_AR$-IgG stimulation in HMEC cells transfected with $ET_AR$ wild type and $ET_AR$ ECL3 Ala. NFAT or SRF activity is depicted relative to NFAT or SRF activity in absence of stimulation, respectively. Data are from eleven (WT) and eight (ECL3) experiments and presented as mean ± SEM, * $p < 0.05$, ** $p < 0.01$, *** $p < 0.005$.

# 5 Discussion

In this work, involvement of the Endothelin-1 type A receptor ($ET_AR$) extracellular loops in the receptor activation and resulting intracellular signaling was investigated. IgG binding to $ET_AR$ triggered a stronger activation of $G_{q/11}$ and $G_{12/13}$ signaling pathways as the natural peptide agonist ET-1. GPCR activation assay in yeasts using mutations of the extracellular loops of the receptor demonstrated that disturbing the third ECL structure might constitutively activate the receptor. Similar results were obtained in mammalian cells, where mutating ECL3 resulted in the constitutive binding of $G_{q/11}$ and $G_{12/13}$ to $ET_AR$. Furthermore, changes in ECL1 structure had only a small impact on $ET_AR$-mediated $G_{q/11}$ pathway activation. On the other hand, without preservation of ECL1 structure, $ET_AR$-triggered $G_{12/13}$ activation after stimulation with ET-1 was lost. Replacement of the second extracellular loop of the receptor by ECL2 of $AT_1R$ confirmed that this domain is only involved in ET-1 induced $G_{12/13}$ pathway activation. These results shed light on the influence of the extracellular loops on $ET_AR$ activation and show that antibodies bind to the receptor in a completely different way than the peptide agonist.

*Yeast GPCR activation assays, applications and models*

In this project, a yeast model was used to assess GPCR activation. The yeast mating pathway is often used to study GPCR activation and signal transduction. The yeast's growth depends on activation of one single GPCR which can be replaced by a mammalian GPCR, which then activates a preserved pathway [52], providing an eukaryotic assay system with no other endogenous responses [51]. To activate the mating pathway, GPCRs must be coupled to a heterotrimeric G-protein consisting of $G_\alpha$ (Gpa1), $G_\beta$ and $G_\gamma$. Compatibility between the receptor and the G-proteins depends on the C-terminus of the $G_\alpha$ subunit. It has been shown that the chimeric $G_\alpha$ subunit consisting of five C-terminal amino acids of a human G-protein fused with the yeast G-protein alters the specificity of $G_\alpha$ without disturbing the signal transduction [49]. Yeast $G_\beta$ and $G_\gamma$ are homologous to mammalian $G_\beta$ and $G_\gamma$ subunits, so that yeast $G_{\beta\gamma}$ may have close structural and functional similarities with mammalian $G_{\beta\gamma}$ subunits [53]. When an agonist binds to a receptor, the

$G_{\beta\gamma}$ subunit transduces signals to the mitogen-activated protein kinase (MAPK) cascade, resulting in cell cycle arrest and gene expression, as *FUS1* for mating. The MMY system used in this study is based on the *Saccharomyces cerevisiae* strain that uses *FUS1* as a pheromone-responsive promoter and the *HIS3* gene as a reporter. *HIS3* encoding the key enzyme that produces histidine, an essential amino acid for yeast growth, is located behind the *FUS1* promoter. As a result, only the cells, in which the human GPCR is activated, can grow in histidine-free selective medium. Experiments have already been performed in the MMY system to study different GPCRs. The role of the second and third extracellular loops of the adenosine $A_1$ receptor was studied using the MMY24 strain, which expresses chimeric Gpa1/$G_{\alpha i3}$. By Means of Alanine scan, the authors demonstrated a strong regulatory role for the ECL2 and the importance of many residues of ECL2 and ECL3 for adenosine $A_1$ receptor activation [54]. Furthermore, adenosine $A_{2B}$ receptor was investigated in the MMY24 strain. Random mutagenesis was introduced in transmembrane domains four and five. The screening identified 22 single and double mutant receptors showing constitutive activity and decreased agonist potency [55]. Many features of the MMY model enable rapid analysis of structural and functional aspects of GPCRs. However, this is not the only existing yeast model to study GPCRs. One of the difficulties in using the yeast system to analyze the signaling of human GPCR is that the coupling between a yeast G-protein and a human GPCR can be ineffective and results in poor signal transduction. Hence, Fukuda *et al.* described a novel strategy for increasing the sensitivity of agonist-mediated signal transduction of human GPCR expressing yeast [56]. Stimulation of ligand induces the expression of both GFP, a reporter gene, and $G_\beta$ gene. Overexpressed $G_\beta$ competes with endogenous $G_\beta$ present in the $G_{\alpha\beta\gamma}$ heterotrimer for $G_\alpha$ binding, wherein the free $G_{\beta\gamma}$ complex can further activate the MAPK cascade and amplify the signal. In parallel, Li *et al.* described a novel yeast genetic screen that only selects for mutant receptors containing inactivation point mutations that is capable of identifying single-point mutations that abolish the receptor function [57]. The yeast strain contains the pheromone-sensitive *FUS2-CAN1* reporter gene encoding the cytotoxic arginine-canavanine permease. Yeasts expressing a functional receptor in the presence of an agonist will not grow, while yeasts expressing a mutant containing inactivating point mutation in a medium containing both carbachol

and canavanine will grow.

*Constitutively active mutants (CAMs) of GPCRs*

Using the MMY yeast model, binding of $ET_AR$-IgG to the extracellular domains of $ET_AR$ was observed. Interestingly, mutation of ECL3 led to a constitutive activation of $ET_AR$. Constitutive receptor activation is defined as the spontaneous formation of a signaling conformation of a receptor, resulting in the production of a second messenger without agonist binding [58]. ECL3 is usually a short loop, so it can constrain TM6 and TM7, limiting their movement and maintaining the receptor's ground state [59]. Substitution in ECL3 relieves this limitation and may affect the conversion of ground state into active state [59]. The ECL3 of $\beta_2$-adrenergic receptor ($\beta_2$AR) replaced by the ECL3 of the $\alpha_{1a}$AR, has a higher binding affinity to agonists and a higher agonist-independent basic adenylyl cyclase activity compared to the wild type $\beta_2$AR, with no influence on the affinity to antagonist [60]. In contrast, replacement of the ECL3 of the TSHR by the ECL3 of the $\beta_2$AR did not affect the basal signaling, but decreased the potency and extent of the TSH-stimulated cAMP response [61]. Other constitutive mutations have been described in GPCRs. The mutation of $Asn295^{7.46}$ to Ala was involved in the constitutive activation of $AT_1R$, probably due to the disruption of two hydrogen bonds between $Asn295^{7.46}$ and $Asn111^{3.35}$, which stabilize the inactive conformation [62]. Asn111 in TM3 helix plays a central role in $AT_1R$ activation through direct interaction with the $Tyr^4$ side chain of Ang II [63].

*Role of ECL1 and ECL2 in other GPCRs*

Further new insights from thesis work are that ECL1 and ECL2 of $ET_AR$ are necessary for ET-1-induced intracellular signaling activation. Crystal structure of Endothelin-1 type B receptor was recently published [11]. As $ET_AR$ and $ET_BR$ vary a lot in their amino acid sequences, it is difficult to draw conclusions from this structure. However, some studies showed the importance of these two ECLs in ET-1 binding to the $ET_A$ receptor. Substitution of ECL1 of $ET_AR$ with the $ET_B$ counterparts significantly reduced the antagonist binding of BQ-123, indicating that the ECL1 is important for binding [64]. Mutations of Gly97, Lys140, Lys159, Gln165 and Phe315, each

located in TM 1,2,3,3 and 6, result in decreased radio-ligand binding to receptor, which has similar levels expressed in cells [13]. In contrast to its involvement in ET-1 binding, mutational studies indicated that ECL2 is not involved in the binding of IgG to $ET_AR$. This is different to other studies on GPCRs and antibodies. Magnusson *et al.* demonstrated that the specific target of stimulatory autoantibodies in patients with dilative cardiomyopathy was the second extracellular loop of the $\beta_1AR$ [65]. Chiale *et al.* confirmed the finding that the autoantibodies bind to the second extracellular loop of the $\beta_1AR$, and they identified agonistic autoantibodies to $\beta_2AR$ [66]. In addition, Unal *et al.* demonstrated that the conformational kinetics of the ECL2 of $AT_1R$ produce an epitope for $AT_1R$ autoantibodies [67]. This allows the antibodies to bind and stabilize the active state of $AT_1R$. Epitope mapping studies in human $AT_1R$ revealed that autoantibodies in patients with preeclampsia bind to epitope "AFHYESQ", the autoantibodies in patients with malignant hypertension and refractory vascular allograft rejection recognize and bind to are epitopes "ENTNIT" and "AFHYESQ" [68].

*Putative pathogenic mechanisms for $G_{q/11}$ and $G_{12/13}$ activation*

Interestingly, antibodies binding to the $ET_AR$ elicited a much stronger $G_{q/11}$ and $G_{12/13}$ activation compared to the binding of the peptide agonist ET-1. This could be responsible for many aspects of pathophysiology of systemic sclerosis. SSc is characterized by abnormal vascular alterations, endothelial cell injury considered as a crucial initiating event leading to vascular remodeling. It has been shown that dysregulation of apoptosis is associated with this process [69]. Apoptosis is a highly conserved cellular mechanism characterized by cell shrinkage, chromatin condensation and nuclear fragmentation. It occurs under many physiological and pathophysiological conditions [70]. Increased endothelial apoptosis has been shown to represent the earliest microvascular abnormality in SSc animal models, suggesting that endothelial cell apoptosis is the initial trigger [71] [72]. Endothelial cell apoptosis has been observed under various pathogenic conditions *in vivo* and can be induced *in vitro* by anti-endothelial cell antibodies in systemic sclerosis [73] [74]. Apoptosis in HeLa cell can be induced by overexpression of active $G_{q/11}$ or stimulation of $M_1$ muscarinic acetylcholine receptor [75]. One study confirmed the importance of $G_{q/11}$ and PKC in

Angiotensin II-induced myocyte apoptosis [76]. The MAP kinase pathway is also involved in the regulation of apoptosis. Two related MAPK kinases, apoptosis signal-regulation kinase 1 (ASK1) and MAPK kinase kinase 1 (MEKK1), stimulate c-Jun kinase (JNK) activity and induce apoptosis. In COS-7 cells, $G_{12/13}$ stimulated the JNK pathway in an ASK-1 and MEKK1-dependent manner during apoptosis [77]. ET-1 may also promote the proliferation of vascular smooth muscle cells and fibroblasts, causing vascular wall thickening [78] [79]. $AT_1R$-IgG and $ET_AR$-IgG specifically bind to their receptors on endothelial cells, induce phosphorylation of ERK1/2 and increase the gene expression of TGF-β, indicating their potential involvement in fibrosis [35]. This process could involve $G_{12/13}$. The $G_{12/13}$ subfamily is of great significance in mediating signaling pathways such as Rho/Rho-associated protein kinase (ROCK)-dependent formation of actin stress fibers [80] and in vascular smooth muscle cell contraction [81], suggesting that the $G_{12/13}$ subfamily may play a considerable role in various physiological effects ET-1 induced such as cell growth, migration, transformation and gene expression.

The results generated in this work show the involvement of the first and second extracellular loops of Endothelin-1 type A receptor in ET-1-induced receptor activation. On the contrary, binding of $ET_AR$-IgG does not rely on the presence of intact ECL1 to 3 and activates $G_{q/11}$ and $G_{12/13}$ more strongly than ET-1. Further studies are required to determine if other extracellular domains of $ET_AR$, like the N-terminus, are involved in the binding of the antibodies to the receptor. These results constitute the first step towards a better understanding of $ET_AR$ immune activation and towards designing new drugs able to impair it specifically.

# 6 References


1. Fredriksson R, Lagerstrom MC, Lundin LG, and Schioth HB, *The G-protein-coupled receptors in the human genome form five main families. Phylogenetic analysis, paralogon groups, and fingerprints.* Mol Pharmacol, 2003. **63**(6): p. 1256-72.
2. Vilardaga JP, Jean-Alphonse FG, and Gardella TJ, *Endosomal generation of cAMP in GPCR signaling.* Nat Chem Biol, 2014. **10**(9): p. 700-6.
3. Davenport AP, Hyndman KA, Dhaun N, Southan C, Kohan DE, Pollock JS, Pollock DM, Webb DJ, and Maguire JJ, *Endothelin.* Pharmacological Reviews, 2016. **68**(2): p. 357-418.
4. Hori S, Komatsu Y, Shigemoto R, Mizuno N, and Nakanishi S, *Distinct tissue distribution and cellular localization of two messenger ribonucleic acids encoding different subtypes of rat endothelin receptors.* Endocrinology, 1992. **130**(4): p. 1885-95.
5. Mayes MD, *Endothelin and endothelin receptor antagonists in systemic rheumatic disease.* Arthritis Rheum, 2003. **48**(5): p. 1190-9.
6. Cyr C, Huebner K, Druck T, and Kris R, *Cloning and chromosomal localization of a human endothelin ETA receptor.* Biochem Biophys Res Commun, 1991. **181**(1): p. 184-90.
7. Horstmeyer A, Cramer H, Sauer T, Muller-Esterl W, and Schroeder C, *Palmitoylation of endothelin receptor A. Differential modulation of signal transduction activity by post-translational modification.* J Biol Chem, 1996. **271**(34): p. 20811-9.
8. Hashido K, Gamou T, Adachi M, Tabuchi H, Watanabe T, Furuichi Y, and Miyamoto C, *Truncation of N-terminal extracellular or C-terminal intracellular domains of human ETA receptor abrogated the binding activity to ET-1.* Biochem Biophys Res Commun, 1992. **187**(3): p. 1241-8.
9. Horinouchi T, Asano H, Higa T, Nishimoto A, Nishiya T, Muramatsu I, and Miwa S, *Differential coupling of human endothelin type A receptor to G(q/11) and G(12) proteins: the functional significance of receptor expression level in generating multiple receptor signaling.* J Pharmacol Sci, 2009. **111**(4): p. 338-51.
10. Schneider MP, Boesen EI, and Pollock DM, *Contrasting actions of endothelin ET(A) and ET(B) receptors in cardiovascular disease.* Annu Rev Pharmacol Toxicol, 2007. **47**: p. 731-59.
11. Shihoya W, Nishizawa T, Okuta A, Tani K, Dohmae N, Fujiyoshi Y, Nureki O, and Doi T, *Activation mechanism of endothelin ETB receptor by endothelin-1.* Nature, 2016. **537**(7620): p. 363-368.
12. Heydenreich FM, Vuckovic Z, Matkovic M, and Veprintsev DB, *Stabilization of G protein-coupled receptors by point mutations.* Front Pharmacol, 2015. **6**: p. 82.
13. Breu V, Hashido K, Broger C, Miyamoto C, Furuichi Y, Hayes A, Kalina B, Loffler BM, Ramuz H, and Clozel M, *Separable binding sites for the natural agonist endothelin-1 and the non-peptide antagonist bosentan on human endothelin-A receptors.* Eur

J Biochem, 1995. **231**(1): p. 266-70.
14. Juan CC, Au LC, Yang FY, Yang DM, and Ho LT, *An endothelin type A receptor-expressing cell to characterize endothelin-1 binding and screen antagonist.* Anal Biochem, 2008. **379**(1): p. 27-31.
15. Lee JA, Elliott JD, Sutiphong JA, Friesen WJ, Ohlstein EH, Stadel JM, Gleason JG, and Peishoff CE, *Tyr-129 Is Important to the Peptide Ligand Affinity and Selectivity of Human Endothelin Type-a Receptor.* Proceedings of the National Academy of Sciences of the United States of America, 1994. **91**(15): p. 7164-7168.
16. Arai H, Nakao K, Takaya K, Hosoda K, Ogawa Y, Nakanishi S, and Imura H, *The human endothelin-B receptor gene. Structural organization and chromosomal assignment.* J Biol Chem, 1993. **268**(5): p. 3463-70.
17. Mazzuca MQ and Khalil RA, *Vascular Endothelin Receptor Type B: Structure, Function and Dysregulation in Vascular Disease.* Biochemical Pharmacology, 2012. **84**(2): p. 147-162.
18. Abraham D and Dashwood M, *Endothelin—role in vascular disease.* Rheumatology, 2008. **47**(suppl_5): p. v23-v24.
19. Dhaun N, Pollock DM, Goddard J, and Webb DJ, *Selective and mixed endothelin receptor antagonism in cardiovascular disease.* Trends Pharmacol Sci, 2007. **28**(11): p. 573-9.
20. Yanagisawa M, Kurihara H, Kimura S, Tomobe Y, Kobayashi M, Mitsui Y, Yazaki Y, Goto K, and Masaki T, *A novel potent vasoconstrictor peptide produced by vascular endothelial cells.* Nature, 1988. **332**(6163): p. 411-5.
21. Shiba R, Yanagisawa M, Miyauchi T, Ishii Y, Kimura S, Uchiyama Y, Masaki T, and Goto K, *Elimination of intravenously injected endothelin-1 from the circulation of the rat.* J Cardiovasc Pharmacol, 1989. **13 Suppl 5**: p. S98-101; discussion S102.
22. Maguire JJ and Davenport AP, *Endothelin Receptors and Their Antagonists.* Seminars in Nephrology, 2015. **35**(2): p. 125-136.
23. Maguire JJ and Davenport AP, *Endothelin Receptors and Their Antagonists()().* Seminars in Nephrology, 2015. **35**(2): p. 125-136.
24. Rubanyi GM and Polokoff MA, *Endothelins: molecular biology, biochemistry, pharmacology, physiology, and pathophysiology.* Pharmacol Rev, 1994. **46**(3): p. 325-415.
25. Kohan DE, Inscho EW, Wesson D, and Pollock DM, *Physiology of endothelin and the kidney.* Compr Physiol, 2011. **1**(2): p. 883-919.
26. Yang LL, Gros R, Kabir MG, Sadi A, Gotlieb AI, Husain M, and Stewart DJ, *Conditional cardiac overexpression of endothelin-1 induces inflammation and dilated cardiomyopathy in mice.* Circulation, 2004. **109**(2): p. 255-61.
27. Coffman L, Mooney C, Lim J, Bai S, Silva I, Gong Y, Yang K, and Buckanovich RJ, *Endothelin receptor-A is required for the recruitment of antitumor T cells and modulates chemotherapy induction of cancer stem cells.* Cancer Biology & Therapy, 2013. **14**(2): p. 184-192.
28. Tam JP, Liu W, Zhang JW, Galantino M, Bertolero F, Cristiani C, Vaghi F, and de

Castiglione R, *Alanine scan of endothelin: importance of aromatic residues.* Peptides, 1994. **15**(4): p. 703-8.
29. Shihoya W, Nishizawa T, Okuta A, Tani K, Dohmae N, Fujiyoshi Y, Nureki O, and Doi T, *Activation mechanism of endothelin ETB receptor by endothelin-1.* Nature, 2016. **537**: p. 363.
30. Nelson J, Bagnato A, Battistini B, and Nisen P, *The endothelin axis: emerging role in cancer.* Nature Reviews Cancer, 2003. **3**: p. 110.
31. Kedzierski RM and Yanagisawa M, *Endothelin system: the double-edged sword in health and disease.* Annu Rev Pharmacol Toxicol, 2001. **41**: p. 851-76.
32. Banasik M, Boratynska M, Koscielska-Kasprzak K, Kaminska D, Zmonarski S, Mazanowska O, Krajewska M, Bartoszek D, Zabinska M, Myszka M, Kaminska M, Halon A, Dawiskiba T, Szyber P, Sas A, and Klinger M, *Non-HLA antibodies: angiotensin II type 1 receptor (anti-AT1R) and endothelin-1 type A receptor (anti-ETAR) are associated with renal allograft injury and graft loss.* Transplant Proc, 2014. **46**(8): p. 2618-21.
33. Banasik M, Boratyńska M, Kościelska-Kasprzak K, Krajewska M, Mazanowska O, Kamiński D, Bartoszek D, Żabińska M, Myszka M, Nowakowska B, Hałoń A, Dawiskiba T, Chudoba P, and Klinger M, *The impact of non-HLA antibodies directed against endothelin-1 type A receptors (ETAR) on early renal transplant outcomes.* Transplant Immunology, 2014. **30**(1): p. 24-29.
34. Hiemann NE, Meyer R, Wellnhofer E, Schoenemann C, Heidecke H, Lachmann N, Hetzer R, and Dragun D, *Non-HLA antibodies targeting vascular receptors enhance alloimmune response and microvasculopathy after heart transplantation.* Transplantation, 2012. **94**(9): p. 919-24.
35. Riemekasten G, Philippe A, Nather M, Slowinski T, Muller DN, Heidecke H, Matucci-Cerinic M, Czirjak L, Lukitsch I, Becker M, Kill A, van Laar JM, Catar R, Luft FC, Burmester GR, Hegner B, and Dragun D, *Involvement of functional autoantibodies against vascular receptors in systemic sclerosis.* Ann Rheum Dis, 2011. **70**(3): p. 530-6.
36. Matucci-Cerinic M, Steen V, Nash P, and Hachulla E, *The complexity of managing systemic sclerosis: screening and diagnosis.* Rheumatology (Oxford), 2009. **48 Suppl 3**: p. iii8-13.
37. Denton CP, Lapadula G, Mouthon L, and Muller-Ladner U, *Renal complications and scleroderma renal crisis.* Rheumatology (Oxford), 2009. **48 Suppl 3**: p. iii32-5.
38. Geyer M and Muller-Ladner U, *The pathogenesis of systemic sclerosis revisited.* Clin Rev Allergy Immunol, 2011. **40**(2): p. 92-103.
39. Hinchcliff M and Varga J, *Obliterative vasculopathy in systemic sclerosis: endothelial precursor cells as novel targets for therapy.* Expert Rev Clin Immunol, 2007. **3**(1): p. 11-5.
40. Hinchcliff M and Varga J, *Obliterative vasculopathy in systemic sclerosis: endothelial precursor cells as novel targets for therapy.* Expert Review of Clinical Immunology,

2007. **3**(1): p. 11-15.
41. Prescott RJ, Freemont AJ, Jones CJ, Hoyland J, and Fielding P, *Sequential dermal microvascular and perivascular changes in the development of scleroderma.* J Pathol, 1992. **166**(3): p. 255-63.
42. Manetti M, Guiducci S, Ibba-Manneschi L, and Matucci-Cerinic M, *Mechanisms in the loss of capillaries in systemic sclerosis: angiogenesis versus vasculogenesis.* Journal of Cellular and Molecular Medicine, 2010. **14**(6a): p. 1241-1254.
43. Vancheeswaran R, Magoulas T, Efrat G, Wheeler-Jones C, Olsen I, Penny R, and Black CM, *Circulating endothelin-1 levels in systemic sclerosis subsets--a marker of fibrosis or vascular dysfunction?* J Rheumatol, 1994. **21**(10): p. 1838-44.
44. Jimenez SA and Derk CT, *FOllowing the molecular pathways toward an understanding of the pathogenesis of systemic sclerosis.* Annals of Internal Medicine, 2004. **140**(1): p. 37-50.
45. Kobayashi H, Nishimaki T, Kaise S, Suzuki T, Watanabe K, Kasukawa R, and Suzuki T, *Immunohistological study endothelin-1 and endothelin-A and B receptors in two patients with scleroderma renal crisis.* Clin Rheumatol, 1999. **18**(5): p. 425-7.
46. Denton CP, Pope JE, Peter HH, Gabrielli A, Boonstra A, van den Hoogen FH, Riemekasten G, De Vita S, Morganti A, Dolberg M, Berkani O, Guillevin L, Scleroderma TRUiPaw, and Connective Tissue Diseases I, *Long-term effects of bosentan on quality of life, survival, safety and tolerability in pulmonary arterial hypertension related to connective tissue diseases.* Ann Rheum Dis, 2008. **67**(9): p. 1222-8.
47. Gunther J, Kill A, Becker MO, Heidecke H, Rademacher J, Siegert E, Radic M, Burmester GR, Dragun D, and Riemekasten G, *Angiotensin receptor type 1 and endothelin receptor type A on immune cells mediate migration and the expression of IL-8 and CCL18 when stimulated by autoantibodies from systemic sclerosis patients.* Arthritis Res Ther, 2014. **16**(2): p. R65.
48. Becker MO, Kill A, Kutsche M, Guenther J, Rose A, Tabeling C, Witzenrath M, Kuhl AA, Heidecke H, Ghofrani HA, Tiede H, Schermuly RT, Nickel N, Hoeper MM, Lukitsch I, Gollasch M, Kuebler WM, Bock S, Burmester GR, Dragun D, and Riemekasten G, *Vascular receptor autoantibodies in pulmonary arterial hypertension associated with systemic sclerosis.* Am J Respir Crit Care Med, 2014. **190**(7): p. 808-17.
49. Olesnicky NS, Brown AJ, Dowell SJ, and Casselton LA, *A constitutively active G-protein-coupled receptor causes mating self-compatibility in the mushroom Coprinus.* EMBO J, 1999. **18**(10): p. 2756-63.
50. Brown AJ, Dyos SL, Whiteway MS, White JHM, Watson M-AEA, Marzioch M, Clare JJ, Cousens DJ, Paddon C, Plumpton C, Romanos MA, and Dowell SJ, *Functional coupling of mammalian receptors to the yeast mating pathway using novel yeast/mammalian G protein α-subunit chimeras.* Yeast, 2000. **16**(1): p. 11-22.
51. Dowell SJ and Brown AJ, *Yeast assays for G protein-coupled receptors.* Methods Mol Biol, 2009. **552**: p. 213-29.
52. Brown AJ, Dyos SL, Whiteway MS, White JH, Watson MA, Marzioch M, Clare JJ, Cousens DJ, Paddon C, Plumpton C, Romanos MA, and Dowell SJ, *Functional*

*coupling of mammalian receptors to the yeast mating pathway using novel yeast/mammalian G protein alpha-subunit chimeras*. Yeast, 2000. **16**(1): p. 11-22.
53. Dowell SJ, Bishop AL, Dyos SL, Brown AJ, and Whiteway MS, *Mapping of a yeast G protein betagamma signaling interaction.* Genetics, 1998. **150**(4): p. 1407-17.
54. Peeters MC, Wisse LE, Dinaj A, Vroling B, Vriend G, and Ijzerman AP, *The role of the second and third extracellular loops of the adenosine A1 receptor in activation and allosteric modulation.* Biochem Pharmacol, 2012. **84**(1): p. 76-87.
55. Peeters MC, Li Q, Elands R, van Westen GJ, Lenselink EB, Muller CE, and AP IJ, *Domains for activation and inactivation in G protein-coupled receptors--a mutational analysis of constitutive activity of the adenosine A2B receptor.* Biochem Pharmacol, 2014. **92**(2): p. 348-57.
56. Fukuda N, Ishii J, Kaishima M, and Kondo A, *Amplification of agonist stimulation of human G-protein-coupled receptor signaling in yeast.* Anal Biochem, 2011. **417**(2): p. 182-7.
57. Li B, Scarselli M, Knudsen CD, Kim SK, Jacobson KA, McMillin SM, and Wess J, *Rapid identification of functionally critical amino acids in a G protein-coupled receptor.* Nat Methods, 2007. **4**(2): p. 169-74.
58. Parnot C, Miserey-Lenkei S, Bardin S, Corvol P, and Clauser E, *Lessons from constitutively active mutants of G protein-coupled receptors.* Trends in Endocrinology & Metabolism, 2002. **13**(8): p. 336-343.
59. Lawson Z and Wheatley M, *The third extracellular loop of G-protein-coupled receptors: more than just a linker between two important transmembrane helices*. Biochem Soc Trans, 2004. **32**(Pt 6): p. 1048-50.
60. Zhao MM, Gaivin RJ, and Perez DM, *The third extracellular loop of the beta2-adrenergic receptor can modulate receptor/G protein affinity.* Mol Pharmacol, 1998. **53**(3): p. 524-9.
61. Kosugi S and Mori T, *The third exoplasmic loop of the thyrotropin receptor is partially involved in signal transduction.* FEBS Lett, 1994. **349**(1): p. 89-92.
62. Zhang H, Han GW, Batyuk A, Ishchenko A, White KL, Patel N, Sadybekov A, Zamlynny B, Rudd MT, Hollenstein K, Tolstikova A, White TA, Hunter MS, Weierstall U, Liu W, Babaoglu K, Moore EL, Katz RD, Shipman JM, Garcia-Calvo M, Sharma S, Sheth P, Soisson SM, Stevens RC, Katritch V, and Cherezov V, *Structural basis for selectivity and diversity in angiotensin II receptors*. Nature, 2017. **544**(7650): p. 327-332.
63. Unal H and Karnik SS, *Constitutive activity in the angiotensin II type 1 receptor: discovery and applications*. Adv Pharmacol, 2014. **70**: p. 155-74.
64. Adachi M, Yang YY, Trzeciak A, Furuichi Y, and Miyamoto C, *Identification of a domain of ETA receptor required for ligand binding.* FEBS Lett, 1992. **311**(2): p. 179-83.
65. Magnusson Y, Marullo S, Hoyer S, Waagstein F, Andersson B, Vahlne A, Guillet JG, Strosberg AD, Hjalmarson A, and Hoebeke J, *Mapping of a functional autoimmune epitope on the beta 1-adrenergic receptor in patients with idiopathic dilated cardiomyopathy.* J Clin Invest, 1990. **86**(5): p. 1658-63.
66. Chiale PA, Rosenbaum MB, Elizari MV, Hjalmarson A, Magnusson Y, Wallukat G, and

Hoebeke J, *High prevalence of antibodies against beta 1- and beta 2-adrenoceptors in patients with primary electrical cardiac abnormalities.* J Am Coll Cardiol, 1995. **26**(4): p. 864-9.

67. Unal H, Jagannathan R, Bhat MB, and Karnik SS, *Ligand-specific conformation of extracellular loop-2 in the angiotensin II type 1 receptor.* J Biol Chem, 2010. **285**(21): p. 16341-50.
68. Dragun D, Muller DN, Brasen JH, Fritsche L, Nieminen-Kelha M, Dechend R, Kintscher U, Rudolph B, Hoebeke J, Eckert D, Mazak I, Plehm R, Schonemann C, Unger T, Budde K, Neumayer HH, Luft FC, and Wallukat G, *Angiotensin II type 1-receptor activating antibodies in renal-allograft rejection.* N Engl J Med, 2005. **352**(6): p. 558-69.
69. Mostmans Y, Cutolo M, Giddelo C, Decuman S, Melsens K, Declercq H, Vandecasteele E, De Keyser F, Distler O, Gutermuth J, and Smith V, *The role of endothelial cells in the vasculopathy of systemic sclerosis: A systematic review.* Autoimmun Rev, 2017. **16**(8): p. 774-786.
70. Cohen JJ, *Apoptosis.* Immunol Today, 1993. **14**(3): p. 126-30.
71. Sgonc R, Gruschwitz MS, Dietrich H, Recheis H, Gershwin ME, and Wick G, *Endothelial cell apoptosis is a primary pathogenetic event underlying skin lesions in avian and human scleroderma.* J Clin Invest, 1996. **98**(3): p. 785-92.
72. Laplante P, Raymond MA, Gagnon G, Vigneault N, Sasseville AM, Langelier Y, Bernard M, Raymond Y, and Hebert MJ, *Novel fibrogenic pathways are activated in response to endothelial apoptosis: implications in the pathophysiology of systemic sclerosis.* J Immunol, 2005. **174**(9): p. 5740-9.
73. Jun JB, Kuechle M, Harlan JM, and Elkon KB, *Fibroblast and endothelial apoptosis in systemic sclerosis.* Curr Opin Rheumatol, 2003. **15**(6): p. 756-60.
74. Bordron A, Dueymes M, Levy Y, Jamin C, Leroy JP, Piette JC, Shoenfeld Y, and Youinou PY, *The binding of some human antiendothelial cell antibodies induces endothelial cell apoptosis.* J Clin Invest, 1998. **101**(10): p. 2029-35.
75. Ueda H, Morishita R, Itoh H, Narumiya S, Mikoshiba K, Kato K, and Asano T, *G alpha(11) induces caspase-mediated proteolytic activation of Rho-associated kinase, ROCK-I, in HeLa cells.* Journal of Biological Chemistry, 2001. **276**(45): p. 42527-42533.
76. Kamato D, Thach L, Bernard R, Chan V, Zheng W, Kaur H, Brimble M, Osman N, and Little PJ, *Structure, Function, Pharmacology, and Therapeutic Potential of the G Protein, Galpha/q,11.* Front Cardiovasc Med, 2015. **2**: p. 14.
77. Berestetskaya YV, Faure MP, Ichijo H, and Voyno-Yasenetskaya TA, *Regulation of apoptosis by alpha-subunits of G12 and G13 proteins via apoptosis signal-regulating kinase-1.* J Biol Chem, 1998. **273**(43): p. 27816-23.
78. Hafizi S, Allen SP, Goodwin AT, Chester AH, and Yacoub MH, *Endothelin-1 stimulates proliferation of human coronary smooth muscle cells via the ET(A) receptor and is co-mitogenic with growth factors.* Atherosclerosis, 1999. **146**(2): p. 351-9.
79. Piacentini L, Gray M, Honbo NY, Chentoufi J, Bergman M, and Karliner JS, *Endothelin-1 stimulates cardiac fibroblast proliferation through activation of protein kinase C.* J Mol Cell Cardiol, 2000. **32**(4): p. 565-76.

80. Buhl AM, Johnson NL, Dhanasekaran N, and Johnson GL, *G alpha 12 and G alpha 13 stimulate Rho-dependent stress fiber formation and focal adhesion assembly.* J Biol Chem, 1995. **270**(42): p. 24631-4.
81. Gohla A, Schultz G, and Offermanns S, *Role for G(12)/G(13) in agonist-induced vascular smooth muscle cell contraction.* Circ Res, 2000. **87**(3): p. 221-7.

# Curriculum Vitae

My curriculum vitae does not appear in the electronic version of my paper for reasons of data protection.

# Publications

**Publication 1**: **Wu Sumin**, Wang Yucheng, Zhen Jie, Wang Ying, Gu Ying. Antibacterial Activity of Ru Photosensitizer: An in vitro Study on Pseudomonas Aeruginosa Strains. Chinese Journal of Laser Medicine & Surgery. 2014.

**Publication 2**: **Wu Sumin**，Wang Ying，Gu Ying. Photodynamic Antibacterial Activation Pseudomonas Aeruginosa in Planktonic and Biofilm Culture in vitro. Chinese Journal of Laser Medicine & Surgery. 2014.

**Publication 3**: **Wu Sumin**，Wang Ying，Gu Ying. Photodynamic inactivation of Pseudomonas aeruginosa by Ru complex. Chinese Journal of Microecology. 2013.

**Publication 4**: Wang Y, Zhou Q, Wang Y, Ren J, Zhao H, **Wu S**, Yang J, Luo Y, Wang X, Gu Y, In Vitro Photodynamic Inactivation Effects of Ru(II) Complexes on Clinical Methicillin-resistant *Staphylococcus aureus* Planktonic and Biofilm Cultures. Photochemistry and Photobiology, 2015.

**Publication 5**: Yucheng Wang, Ying Wang, **Sumin Wu** et al, *In vitro* sensitivity of Candida spp. to hematoporphyrin monomethyl ether-mediated photodynamic inactivation, *Proc*. *SPIE* 9268, Optics in Health Care and Biomedical Optics VI, 92680L, 2014.

**Publication 6**: Zhao H, Yin R, Wang Y, Lee YH, Luo T, Zhang J, Qiu H, Ambrose S, Wang L, Ren J, Yao J, Chen D, Wang Y, Liang Z, Zhen J, **Wu S**, Ye Z, Zeng J, Huang N, Gu Y, Modulating mitochondrial morphology enhances antitumor effect of 5-ALA-mediated photodynamic therapy both in vitro and in vivo. J Photochem Photobiol B, 2017.

# Affidavit

“I, Sumin, Wu certify under penalty of perjury by my own signature that I have submitted the thesis on the topic [Structural and functional basis of Endothelin-1 type A receptor ($ET_AR$) activation] I wrote this thesis independently and without assistance from third parties, I used no other aids than the listed sources and resources.

All points based literally or in spirit on publications or presentations of other authors are, as such, in proper citations (see "uniform requirements for manuscripts (URM)" the ICMJE www.icmje.org) indicated. The sections on methodology (in particular practical work, laboratory requirements, statistical processing) and results (in particular images, graphics and tables) correspond to the URM (s.o) and are answered by me. My interest in any publications to this dissertation correspond to those that are specified in the following joint declaration with the responsible person and supervisor. All publications resulting from this thesis and which I am author correspond to the URM (see above) and I am solely responsible.

The importance of this affidavit and the criminal consequences of a false affidavit (section 156,161 of the Criminal Code) are known to me and I understand the rights and responsibilities stated therein.

Date Signature

# Acknowledgement

Studying abroad was my dream from childhood. Thanks to my supervisor, Prof. Duska Dragun, for accepting me as her student, so that I have the opportunity to study and live in Berlin, and to work with so many outstanding scientific researchers. I have had a great time during the three years studying with AG Dragun!

Many thanks to my little boss, Aurelie Philippe, for giving her concerns and care to me. I will never forget that you went to Tegel airport to pick me up on a rainy night; taught me a variety of experimental techniques patiently; even discussed with me about the plans and arrangement after my graduation and so on. All these things reflected your thousand little cares for me, it is really my luck that I have you!

Thank you, Angelika and Rusan, for the guidance on my experiments and valuable suggestions on my thesis. Thanks to Dennis and Marc for the help and concerns. Thanks to Jannis, Ola, Chen Lei, Julia, Ren Peng and Li Qing for the companionship and help. Each of you has a lot of merits that I can learn from!

My dear friends, Zhou Ming and Wang Ye, thanks for your spiritual support, even we are apart from each other for thousand miles. I feel that we will be good friends for a lifetime. Thank you Xiaoyun and Xueyi for taking care of me. It is not easy to have friends like you guys. I will cherish our friendship forever!

Mom and Dad, thank you for being 100% supportive no matter what I decide and do. There is no me, Dr. Wu, without your understanding and support. I can now imagine that you are really proud of me while talking to your friends and colleagues. I love you!

In the past three years, I have received too much help from my parent, relatives, friends and colleagues. I just want to wish you all, those who care about me, happy every day! Thank you thank you!